



**AAiT**

Addis Ababa Institute of Technology  
Addis Ababa University

**Addis Ababa University  
Addis Ababa Institute of Technology  
School of Mechanical and Industrial Engineering**

**EXTENT OF ADHESION LOSSES IN THE WHEEL-  
RAIL CONTACT UNDER CONTAMINATED  
CONDITIONS**

**A Thesis Submitted to the School of Mechanical and Industrial  
Engineering in Partial Fulfillment of the Requirements for the Degree  
of Masters of Science in Mechanical Engineering**

**(Rolling Stock Stream)**

**By: Mesfin G/Tsadik**

**Advisor: Dr. Daniel Tilahun**

**December, 2014**

## ACKNOWLEDGMENT

There are several people and organization that made this thesis possible. In attempting to acknowledge all of them, I'm sure that I will leave some out, but this represents my best attempt to capture them all.

Success of any work of course would not be completed without the help of others. Therefore it is a must to mention the names of the people and express my deep felt gratitude to those contributed most in the work directly or indirectly.

First of all, I would like to express my deep felt gratitude for my adviser, Dr. Daniel Tilhun Redda, for his interest in this thesis subject, for his helpful comments and suggestions and without whose advises, encouragement and patience, this work would not have been possible, even to think of. The suggestions, tips and advises given by friend Nega Girma were immensely helpful in constructing the test machine. I would like to express my sincere thanks to Habamu Tekubet for guiding me and facilitating the budget for the thesis. I would also like to thank the AAIT electrical department staffs in helping me to carry out the Lab test. Especially Ato Amare Asefa, Assistant lecturer, you deserve special thanks for your assistance and guidance on performing the lab test.

I am greatly indebted to Hibiret Manufacturing and Machine Building Industry for sponsoring me to build the twin disc test machine. A lot of people in HIBIRET deserve credit for their support in the construction of this test machine. Captain Solomon, Deputy General Manager and Operation Head of HIBIRET should take the upper hand and is particularly thanked for facilitating every possible means to build the test machine. All the staffs of machine building shop of Hibret are also greatly acknowledged for bringing me a pleasant working environment and for promoting constantly a good working atmosphere. Thanks are surely extended to Atede Tefera, section head PPC, Etana Atomsa, material technician, my nephew Abiy Giday, machinist, Tibebe Tesfaye, team leader and specifically Yonas Birhanu, sub-supervisor of the heavy duty shop contributed most in manufacturing every parts of the test machine amidst his busy schedule. I would also like to thank the rest of the industry's work men to their admirable help whenever they are in need of.

I owe deep and a special thanks to my best friend Ayana Gebremichael for his unreserved co-operations and assistance in performing my thesis. I very much appreciated the assistance of the mechanical work shop staffs of AAIT. Acknowledgement is also due to my colleague Gutenber Dabare for his company and helping each other throughout the time of performing the thesis.

I cannot finish without mentioning my family. This goes beyond the typical Support one would find in an adventure such as this, but included very tangible implications of its success. No one could even consider starting an endeavor such as this without the support and encouragement of my wife Jerry. Nothing would have been possible without her.

Thank you all, and may the adhesive force of life be with you!

Mesfin G/Tsadik, Oct. 2014

## ABSTRACT

Railway vehicles require a certain level of adhesion between wheel and rail to operate efficiently, reliably, and economically. Different levels of adhesion are needed depending on the vehicle running conditions. In the wheel tread–railhead contact, the dominant problem is low adhesion, as low adhesion on the railhead negatively affects railway operation: on one hand, the vehicle will lose traction resulting in delay when driving on low-adhesion tracks; on the other hand, low adhesion during deceleration will extend the braking distance, which is a safety issue.

This thesis examines the influence of several contaminants, i.e., water, mud, leaves, oil and grease, on the adhesion in the wheel tread–railhead contact. This study will also improve our knowledge of the low-adhesion mechanism and of how various contaminants influence adhesion.

In this thesis, the adhesion conditions were assessed using a twin disc test machine. Thus the research methodology used was a laboratory test; the aim of which was to study the extent of adhesion coefficients over a range of slip values with and without contaminants. Thus the outcomes from lab test were the coefficients of adhesions of each contaminant within 0 to 10% slip values so as to sort out which of them are the worst to cause loss of adhesion. With this regard oil and grease have been found to create less adhesion than leaves unlike the researches made abroad so far.

Keywords: Wheel tread–railhead contact; Contaminants; Adhesion; Slip; Twin disc.

# Contents

ACKNOWLEDGMENT.....	i
ABSTRACT.....	iii
LIST OF FIGURES .....	vi
LIST OF TABLES.....	viii
NOMENCLATURE .....	ix
CHAPTER ONE: INTRODUCTION.....	1
1.1. Background of the study.....	1
1.2. Adhesion Force and adhesion coefficient.....	3
1.3. Statement of the Problem.....	5
1.4 Objective of the Research.....	5
1.5 Approach of the Research.....	6
1.6 Scope and Limitations of the Research .....	7
1.7 Organization of the Thesis.....	7
CHAPTER TWO: LITERATURE REVIEW .....	8
2.1. Introduction .....	8
2.2. Theoretical Background.....	9
2.3. Adhesion basics .....	15
2.4. Causes of low adhesion .....	19
2.5. Contamination of contact surface .....	19
2.6. Twin-disc Test apparatus description .....	27
2.7. Specimens/Test discs .....	30
CHAPTER THREE: EXPERIMENTAL METHODS, PROCEDURE, AND CONDITIONS	34

---

3.1. Material.....	34
3.2. Feature and Dimension of the test rigs/Specimen.....	35
3.3. Method and Test Description.....	37
3.3.1 Test set-up and Conditions.....	37
3.3.2. Tested contaminants.....	40
3.4. Test Procedure.....	40
CHAPTERFOUR: RESULTAND DISCUSSION.....	44
4.1 Experimental Results.....	44
4.1.1 Dry tests.....	44
4.1.2 Water test.....	45
4.1.3 Mud test.....	46
4.1.4 Leaf test.....	47
4.1.5 Test with oil.....	48
4.1.6 Test with grease.....	49
4.2 Discussion.....	50
CHAPTER FIVE: CONCLUSION, RECOMMENDATION AND FUTURE WORK.....	53
5.1 Conclusion.....	53
5.2 Recommendation.....	55
5.3 Future Work.....	56
Reference.....	57
Appendix.....	60

## LIST OF FIGURES

Figure 1.1 Schematic representations of the common types of adhesion requirement in Netherlands railway transportation [3] .....	2
Figure 1.2 shows a cylinder rolling along a stationary plane surface. [1] .....	3
Figure 1.3 contact mode of the twin discs [9].....	6
Figure 2.1 how the adhesion between the rail and the wheel varies according to slip [4] .....	10
Figure 2.2 Relationship between adhesions and creep [1, 36].....	11
Figure 2.3 Schematic of the adhesion curve and coefficient of friction under clean and contaminated condition [1] .....	12
Figure 2.4 General curve of traction coefficient in function of slip [6].....	13
Fig 2.6 Creep motion of railway wheel [10].....	15
Figure 2.9 the third-body layer between the bulk materials in the wheel–rail contact [1] .....	22
Figure2.10. Stribeck curve [1, 2, 17] .....	23
Fig 2.11 Concept of partially lubricated contact [10].....	25
Figure2.12 UTM 2000 Twin Disc machine [14] .....	28
Figure 2.13 Amsler twin disc machine [18].....	29
Fig. 2.14 Schematic diagram of the twin disc test machine [3, 10, 20 and 28]. .....	29
Figure 2.16 Wheel and Rail Disc Specimens taken from wheel and rail [8].....	33
Figure 3.1 Feature of the test rig in CATIA V5.....	36
Figure3.3 Photograph of the test discs that are manufactured .....	37
Figure 3.4 Schematic representation of the setup .....	38
Figure 3.5 Photograph of the set-up.....	38
Figure 3.6 Photographs of the contaminants in to consideration for adhesion testing .	40
Figure 3.7 Experimental set up of leaves feeding.....	42
Figure 3.7 Rail and Wheel discs after leaf test with blackish leaf layers .....	43
Figure 4.1 Adhesion tests in dry conditions.....	45
Figure 4.2 Adhesion tests in wet condition conditions .....	46
Figure 4.3 Adhesion tests in muddy conditions.....	47

Figure 4.4 Adhesion tests in wet leaves.....	48
Figure 4.5 Adhesion tests in oil contaminated condition.....	49
Figure 4.6 Adhesion tests of grease as a contaminant .....	50
Figure 4.7.Slip/Creep Curves for the various Test Conditions.....	51

## LIST OF TABLES

Table 1.1 Required adhesion coefficients [1, 2] .....	4
Table 2.1. Friction coefficients measured on metro lines using a hand-pushed tribometer [1]. .....	20
Table 2.2 Examples of wheel–rail adhesion coefficients discussed in [2, 12] .....	21
Table 2.3: Wheel and rail material composition from Yi Zhu [1,2] .....	31
Table 2.4: Test Rig Parameters [21] .....	31
Table 2.5 Mechanical properties of wheel and rail, high carbon steel [22] .....	32
Table 3.1: Material composition of steel wheel and rail steel discs which suit to UIC standard (UIC 900A rail and R7 wheel) and Chinese standard. ....	34
Table 3.2: Mechanical properties of the selected materials for both the wheel and rail disc samples .....	35
Table 4.1 Slip values Vs adhesion coefficient of dry test .....	44
Table 4.2 Slip values Vs adhesion coefficient of water test .....	45
Table 4.3 Slip values Vs adhesion coefficient of mud test .....	46
Table 4.4 Slip values Vs adhesion coefficient of leaf test .....	47
Table 4.5 Slip values Vs adhesion coefficient of oil test .....	48
Table 4.6 Slip values Vs adhesion coefficient of grease test .....	49
Table 4.7 all adhesion data of the contaminants are collected for comparison purpose .....	50

## NOMENCLATURE

UIC: International union of railways

$v$ : Speed of the Vehicle

S: slip ratio

$\omega$ : Angular Velocity of the Wheel

$\omega r$ : circumferential velocity of wheel

$r$ : radius of the wheel

$\sigma_{UTS}$ : Ultimate Tensile Strength

$V_s$ : Slip velocity

$F_a$  : Adhesion force

$F_T$  : tangential force/traction force

$\sigma_y$  : yield strength

$F_N$  : applied normal force

$m_a$  : the adhesive mass of the vehicle

$\mu_a$  : adhesion coefficient

$g$  : the gravitational constant

$\mu_f$  : friction coefficient

$v_1$  and  $v_2$  : the speeds of the contacting bodies

$\mu_{\text{capacity}}$ : full tractive capacity

$\mu_{\text{time table}}$ : time table for traction

$\mu_{\text{safety}}$  : safe braking distance

$V^{\text{rel}}$  : relative velocity of the two discs

$V^{\text{mean}}$  : Mean velocity of the two discs

Na: active number of coil

Ea: Armature voltage

Ia : armature current

Tcalc: calculated Torque from data of armature voltage, armature current rotational speed of the shunt type motor's shaft

T const : Torque calculated from the applied load and radius of the test rig

$\mu_{\text{a calc.}}$  : adhesion coefficient calculated from Tcalc. and Tconst.

# CHAPTER ONE: INTRODUCTION

## 1.1. Background of the study

Since the beginning of railway transportation, wheel-rail adhesion has been limiting the acceleration and deceleration capabilities of rolling stocks. Sliding and slipping have always been major problem in the railway industry due to the low friction between wheel and rail. With increased speed, power and complexity of the modern railway vehicle, sliding and slipping phenomena have been seen to increase abruptly. In recent decades, special attention has been paid to the limitations in adhesion due to the requirement for a more rapid, reliable and denser railway transportation that can satisfy the increasing demand on public transportation. As railway transportation is still characterized by steel wheels and steel rails operating on open system ,the wheel rail contact remains easily contaminated by water, leaves, grease ,mud etc causing railways to suffer from lower adhesion problems. Thus to run such vehicles efficiently and economically, the wheel–rail adhesion should be maintained at a certain level. Adhesion loss affects vehicle performance because the vehicle will lose traction when driving on low-adhesion track. Moreover, low adhesion is also a safety issue, since poor adhesion when decelerating will extend braking distance [1]. Since the wheel–rail contact is an open system, many environmental factors can contribute to low adhesion on the railhead .According to Yi Zhu in [1],in Netherland’s railway transportation, the maximum adhesion requirement are classified as type of vehicle, running speed ,type of contaminants in touch and amount of load per axle .According to the vehicle running conditions wheel–rail contact is generally divided into two categories as wheel tread–railhead contact on straight track which is also main concern of this thesis while the other is wheel flange–rail gauge contact on curved track. In most cases, flange contact requires a low adhesion coefficient to reduce wear and noise, while tread and rail head contact requires a comparatively high adhesion coefficient to obtain good accelerating and decelerating ability.[2]

In this free market world, customer handling have been given a great emphasis. Thus to attract more customers and compete with other modes of transportation, railway transport needs to ensure safety, punctuality, high comfort, and low cost. Wheel–rail adhesion, i.e., the transmitted tangential force in the longitudinal direction during

driving and braking plays an important role in all these aspects. Adhesion thus needs to be kept at a certain level for railway operation and maintenance. However, wheel–rail contact is an open system contact. Different contaminants can present between the wheel and rail surfaces, forming a third-body layer as in figure 2.4 of Yi Zhu [1] that affects the adhesion. Prediction of wheel–rail adhesion is important for railway operations and for research into vehicle dynamics; however, this prediction is difficult because of the presence of contaminants.

The adhesion requirement as to [3] is divided into three main categories i.e. traction /braking capacity of the rolling stock, time table regulations and safety during operation. The figure 1.1 shown below is used to express the common types of adhesion requirements in Dutch railway transportation in which the length of the bar representing proportions of the adhesion requirements. The same holds true for every country's railway company; however, the extent adhesion requirement varies in accordance to the environmental conditions each country in the world has.

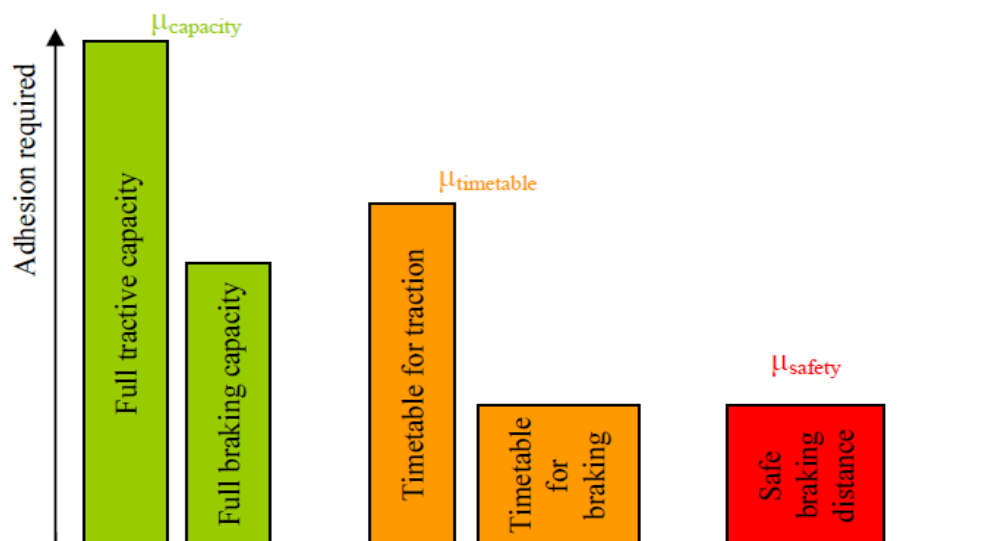


Figure 1.1 Schematic representations of the common types of adhesion requirement in Netherlands railway transportation [3]

It should also be noted that the adhesion coefficient requirements also depend on the type of rolling stock, traction and braking systems, number of powered/braking axles, etc.

## 1.2. Adhesion Force and adhesion coefficient

A general scientific definition of the adhesive force is the force of attachment between two contacting objects. If this definition is translated in to a railway definition as briefly described in [4], it will be the ability of the wheel to exert the maximum traction force on the rail and still maintain persistence of contact without exceeding the optimal slip. Thus adhesion is the amount of force available between the rail and the wheel. Therefore, one can say that the adhesive force comes about as a result of the frictional forces. Further, the friction force is a resistance of motion, and as such an undesirable effect, while adhesion is a coupling force and therefore something desirable. [4]

The adhesive force is given by:

$$F_a = \mu_a F_N = \mu_a m_a g \quad 1.1$$

Where  $F_a$  is the adhesive force,  $\mu_a$  is adhesion coefficient,  $F_N$  is the normal force,  $m_a$  is the adhesive mass of the vehicle and  $g$  is the gravitational constant. The adhesive mass is defined by the total mass on all the driven wheels [4].

The adhesive force  $F_a$  changes in time, though the normal force  $F_N$  is constant, which implies that the adhesion coefficient  $\mu_a$  changes in time. The adhesion coefficient ( $\mu_{\text{adhesion}}$ ) is limited by the friction coefficient ( $\mu_{\text{friction}}$ ), which is defined as in figure 1.2 in [1].

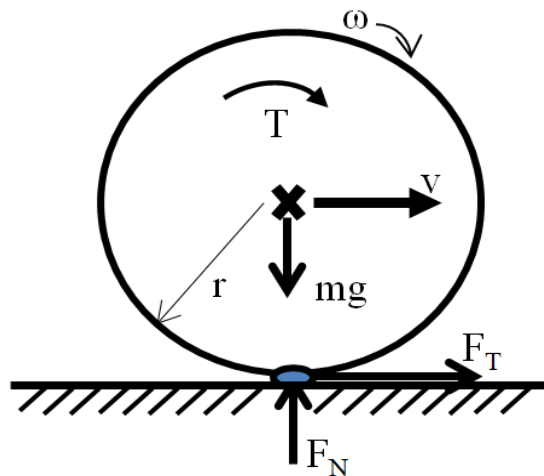


Figure 1.2 shows a cylinder rolling along a stationary plane surface. [1]

This is analogous to the case of a wheel rolling along a rail. The wheel is subject to normal force,  $F_N$  and travels along the rail at velocity  $v$ . The wheel is subject to torque  $T$ , which maintains the angular velocity of the wheel,  $\omega$ , and also causes a reactive tangential force,  $F_T$  at the wheel–rail interface. The tangential force of a driving wheel is known as traction, which ultimately propels the wheel along the rail. During deceleration, the tangential force,  $F_T$  opposes the running direction due to the braking torque,  $T$  applied anticlockwise. The tangential force in the longitudinal direction during both acceleration and deceleration is referred to as adhesion. The ratio between the adhesion force and the normal force is known as the adhesion coefficient [1].

$$\mu_a = \frac{F_T}{F_N} \leq \mu_f \quad 1.2$$

According to field measurements [2] the coefficient of friction is higher on the railhead than on the rail edge. Adhesion coefficient requirements for braking and traction in three countries are described in the table 1.1 by [1, 2]. Despite the environmental conditions each country has, The adhesion requirement depicted in table 1.1 will give some clues for comparison with that of Ethiopian railway transportation system.

Table 1.1 Required adhesion coefficients [1, 2]

	Adhesion coefficient for braking	Adhesion coefficient for traction
Stockholm public transport	Approximately 0.15	0.18
U.K.	0.09	0.2
Netherlands	0.07	0.17

There are several factors that can affect the value of the adhesion coefficient, such as:

- Contaminants
- Vehicle velocity
- Slip velocity and

- Weight of the vehicle

As the main concern of this paper is to investigate the effects of contaminants that cause adhesion losses, it is vital to acquire a better understanding of the adhesion-reduction mechanism of the contaminants in consideration. Contaminants such as water, iron oxide, dust or mud, oil leaking from engine and leaves discussed in [1,2, 3,7, ,8,12] which are unintentionally present on the rail and wheel contact and some of them deliberately applied to the rail edge or wheel corner to prevent wear. These are considered as adhesion depriving contaminants as long as their effects exceed the maximum limit. This is well reviewed in chapter two, in the literature review part.

### **1.3. Statement of the Problem**

Extremely low friction values between the wheel and the rail are reported worldwide, leading to severe delays and sometimes even to accidents. Slippery tracks due to water in the form of rain/drizzle occur at specific times of the year especially in the rainy seasons are expected to cause low adhesion. Oil dripping from leaking trains or deposited at level crossing by vehicle tires or spilt goods will be also expected one of the problem for rail head surface contaminants. Rail service may be also disrupted by fallen leaves crushed eventually forming a hard slippery blackish layer resulting in low adhesion performance measures like cost, time, information flow and quality. Due to this, investigations have to be performed which contaminants are the worst in the reduction of adhesion with the conditions in touch.

### **1.4 Objective of the Research**

#### **1.4.1. General Objective**

The overall goal of this thesis was to investigate the influence of contaminants (i.e., water, mud, oil, leaves and grease) experimentally on the adhesion coefficient in the wheel tread–railhead contact and figuring out the extent of adhesion coefficients of each contaminant under predetermined slip values and compared with that of dry test.

#### **1.4.2. Specific Objective of the Research**

- Prepare both wheel and rail specimens.

- Assess the common contaminants inducing low adhesion in the wheel-rail contact with the context of our environmental condition.
- Conduct the lab test.
- Collect test data and calculate adhesion coefficient.
- Compare the effects contaminants, with each other and with that of the dry test.

## 1.5 Approach of the Research

In order to achieve the primary objective, experimental investigations have been performed. The experimental investigations have been carried out in the laboratory. The laboratory examination was performed with a twin disc roller ring in which the actual wheel-rail contact was simulated by two identical discs that are pushed against each other as in fig 1.3 in rolling-sliding motion. The influences the different types of contaminants (water, mud, leaves, oil and grease) simulating the wheel-rail adhesion conditions have been investigated by two contacting rollers with fixed slip mechanism.

The laboratory test approach has been chosen mainly for two reasons. The first one is field test which is impossible to carry out at this time. The other one is computer simulation is somewhat complicated due to the characteristics of contaminants i.e. viscosity of contaminants should be identified.



Figure 1.3 contact mode of the twin discs [9].

The major problem in the laboratory test with this adhesion test machine is that the results may not be extrapolated to the actual condition due to the differences in geometry and operational conditions. Therefore the laboratory testing can provide a

qualitative indication of what happens in the actual wheel-rail and to identify the more influencing contaminants on adhesion losses.

## **1.6 Scope and Limitations of the Research**

As described in the problem statement there are many contaminants that affect the adhesion between wheel and rail. This thesis mainly investigates the adhesion coefficients of water, mud, leaves, oil and grease which are believed in causing adhesion losses with the context of Ethiopian railway system.

### **1.6.1. Scope of the Experimental Study**

The scope of the experimental study is to investigate the extent of adhesion coefficients of water, mud, track side leaves, oil and grease. From the results attained suggestions and recommendations are the feedbacks to take measures on adhesion problems in the Ethiopian railway transportation system.

### **1.6.2. Limitations of the Research**

- Lack of appropriate motors, torque encoders and force measuring equipment on market were limiting factors to simulate the real contact conditions.
- Lacks of plasma cutting machine lead me in preparing a relatively close material for the specimen of rail and wheel discs.
- It would have been possible to acquire all data on a PC which is also used for load and speed control if servo motors would have been fitted.
- Lack of information from ERC about the technical specifications

## **1.7 Organization of the Thesis**

This paper consists of five chapters. The first chapter deals with the introduction while the second chapter focuses on the review of literatures related to this paper. Chapter three addresses the methods, materials procedures used throughout this thesis .Chapter four comes with the test results and discussions. The next one, i.e. chapter five comprises conclusion, recommendation and future work of the research. The end of the paper will close up with sets of references used throughout the research and an appendix.

## CHAPTER TWO: LITERATURE REVIEW

### 2.1. Introduction

Reviews of literatures revealed the different type of modeling such as mathematical as well as computer simulations are low cost to simulate adhesion loss but also significantly lab testing has been preferably chosen due to resemblance of the wheel-rail contact conditions and was believed to be cost effective as well to simulate the wheel-rail adhesion condition under different contaminants. These referred literatures were journals, conference papers, theses and books related to this paper. The results attained on each reviewed works at the selected conditions, approaches and methodologies were used as a guidance and comparison for outcome of this paper. These reviewed literatures have thus been believed to be the pavement to achieve this thesis work. As to the aim of this thesis, experimental investigations were performed addressing the issue of adhesion losses due to the different contaminants. Not only concerning the adhesion conditions hints of constructing the test machine were grasped from the literatures and of course achieved by constructing the test machine here as a phase one of this thesis.

Based on the literatures reviewed, adhesion losses were seen as serious incidences and adhesion depriving agents were studied thoroughly and decided, water, mud, track side leaves, oil and grease were chosen to test with simulating wheel-rail contact conditions at the actual environmental scenarios. So far researchers abroad made studies on the contaminants which caused adhesion loss during traction as well as braking with regard to their environmental conditions. What about in our condition was the concern of this thesis. To come to a decision to carry out the tests with twin disc test machine constructed here, a lot of references have been sighted to ensure seemingly outcome of the test results. To accustom techniques of knowing of the extent of adhesion experimentally, what do literatures in tell about the different lab test methods, materials and basic concepts in figuring out the adhesion coefficients at different contact conditions was the aim of reviewing the different literature here after.

## 2.2. Theoretical Background

One of the most fundamental theories in vehicle dynamics is the slip theory. A driven wheel does not roll, but actually rotates faster than the corresponding longitudinal velocity of the vehicle. The difference between the angular velocity of the wheel and the corresponding longitudinal velocity causes the slip as Eq.2.1. [4]

$$S = \frac{\omega r - v}{v} \quad 2.1$$

Where  $r$  is the radius of the wheel;  $\omega$  is the angular velocity of the wheel and  $v$  is the longitudinal velocity of the vehicle.

Due to slip/creep, the contact areas are divided into stick and slip regions at the micro-scale level as (Fig. 2.2). When creep is zero, the motion is pure rolling motion and the stick region covers the whole contact area which requires minimum adhesion force. When a tangential force starts to be transmitted, a slip region appears in the contact patch. With increasing creep, the slip region increases and the stick region decreases in size, resulting in a rolling–sliding contact. When creep is great enough, the stick region disappears leading to gross slip and maximizing transmitted tangential force. The maximum tangential force is limited by the friction force available between two surfaces. [4]

### 2.2.1 Slip, Slip Velocity and Slip Curves

#### Slip velocity

The slip velocity, defined in Equation (2.2), is the most important factor influencing adhesion. The adhesion coefficient becomes higher if the slip velocity is controlled effectively [4]. This means that different reference slip velocities should be used depending on the current rail condition. Much experimental work has been done to derive a general relationship for how slip velocity affects the adhesion coefficient, and thereby the adhesive force [4].

$$v_s = \omega r - v \quad 2.2$$

Where  $V_s$  is slip velocity,  $\omega r$  circumferential velocity of wheel and  $v$  is velocity of the vehicle.

## Slip Curves

In a railway vehicle movement, some slip is required in order to transfer the motor torque to vehicle movement. The adhesive force increases when the slip increases, as long as the slip does not become too large. Adhesion coefficient has a peak value at a certain slip velocity as presented in Figure 2.1. In this figure, the region to the left of the peak is referred to as the stable region, while the right side is called the unstable region [4].

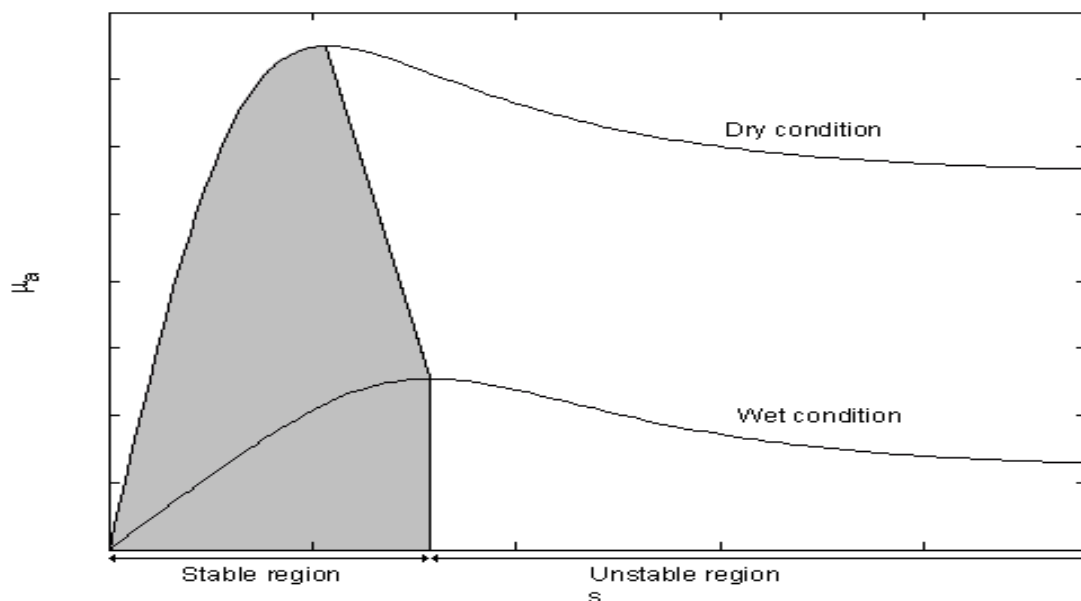


Figure 2.1 how the adhesion between the rail and the wheel varies according to slip [4]

Figure 2.2 in [1, 36] shows the relationship between creep and adhesion for a typical dry wheel–rail contact. This plot of adhesion versus creep is known as the creep curve. When the creep is zero, the whole contact area sticks and no tangential force is transmitted, in what is known as “free rolling”. However, zero creep does not exist in reality, since the inevitable deformation between two contact bodies results in a certain amount of creep. Slip occurs at the trailing edge and spreads forward through to the contact area as the adhesion increases. The slip region increases and the stick region decreases resulting in a rolling–sliding contact until pure sliding appears. In that state, the adhesion equals the friction force between two bodies under pure sliding conditions. When the creep is small, the adhesion increases in an approximately linear fashion with increased creep. After that, the slope of the creep curve (the increasing rate of adhesion) decreases with increased creep. At approximately 1–2% creep, the slope of the creep curve and the stick region are extremely small, and the adhesion is

very close to the friction. For a typical creep curve in the railway context, the adhesion decreases after reaching its maximum, typically at 1–2% creep under dry and clean conditions. The adhesion at that point is considered the maximum tangential force that approximately equals the friction force [1, 2].

During acceleration or when overcoming losses while driving at constant speed, the tangential velocity at the wheel surface,  $\omega r$ , of a driven wheel will always be greater than its body velocity,  $v$ . The difference between the tangential velocity of the wheel,  $\omega r$ , and the body velocity,  $v$ , divided by the rolling velocity is referred to as creep and is usually given as a percentage [1].

Since adhesion is the tangential force in the longitudinal direction, the creep/slip discussed here refers to longitudinal creep/slip and the contact refers to the wheel tread–railhead contact.

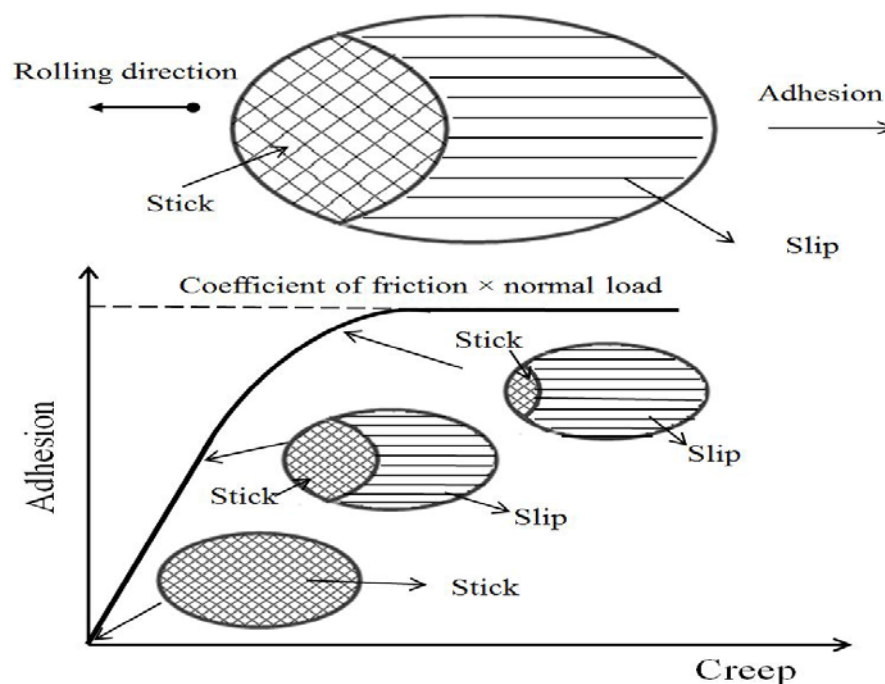


Figure 2.2 Relationship between adhesions and creep [1, 36]

As shown in the figure 2.3, discussed by Yi Zhu in [1] friction coefficient is larger than the adhesion coefficient under both clean and contaminated conditions, although the values under clean conditions are larger than those under contaminated conditions. Note that the friction coefficient shown in the figure is kept constant to enable comparison between the friction and adhesion coefficients; in reality, the coefficient of friction is not constant.

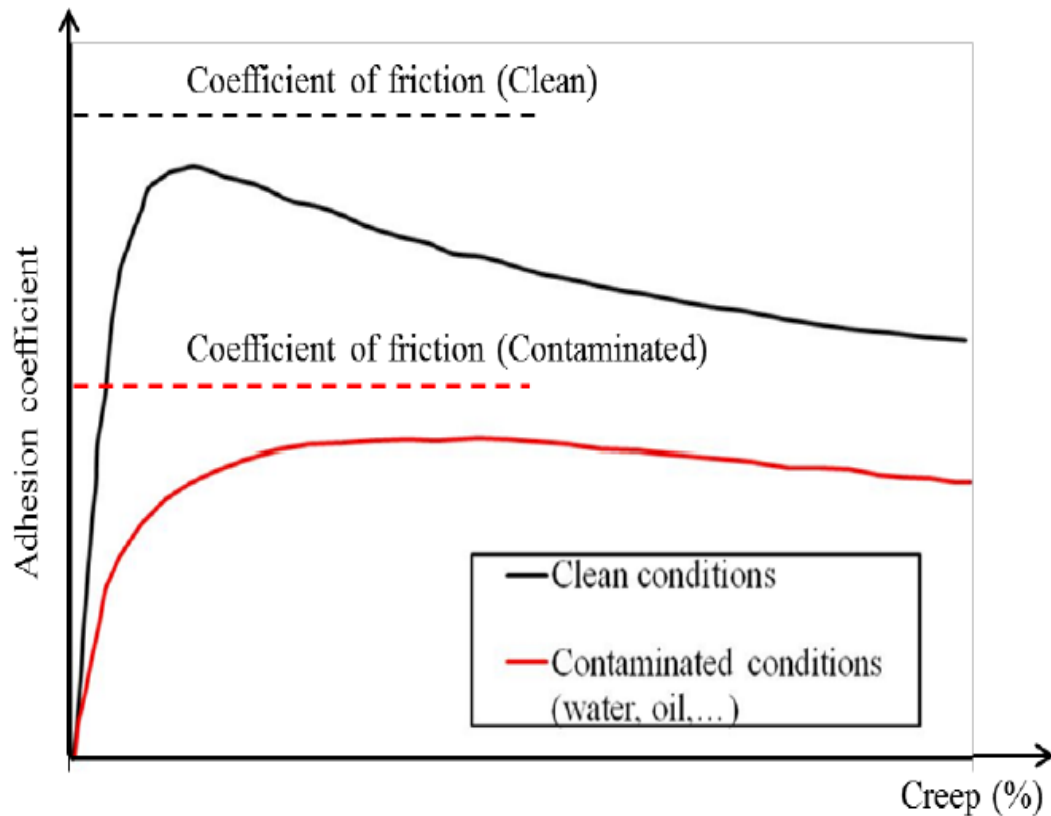


Figure 2.3 Schematic of the adhesion curve and coefficient of friction under clean and contaminated condition [1]

Pure rolling takes place in the contact area when the surface velocity of the two bodies is equal. In the case of two equal cylinders in contact, they must have the same rotational speed. If the circumference velocity is unequal, the rolling motion is accomplished with sliding. If two contacting bodies experience a tangential force  $Q$ , a shear stress will arise in the contact area. No macroscopic sliding takes place if the tangential force is smaller than the limiting friction force  $\mu F$ . From the microscopic point of view, a shear stress  $q$  occurs in the contact area. The distribution of the shear stress is not predictable in advance and has to be found by trial and error, until all the specific boundary conditions are fulfilled [6].

As to [6] traction is often considered as a black box, where only the experimental relation between the traction coefficient and the slip is known (Figure 2.4). The slip  $S$  is defined as the ratio between the sliding velocity and the mean velocity.

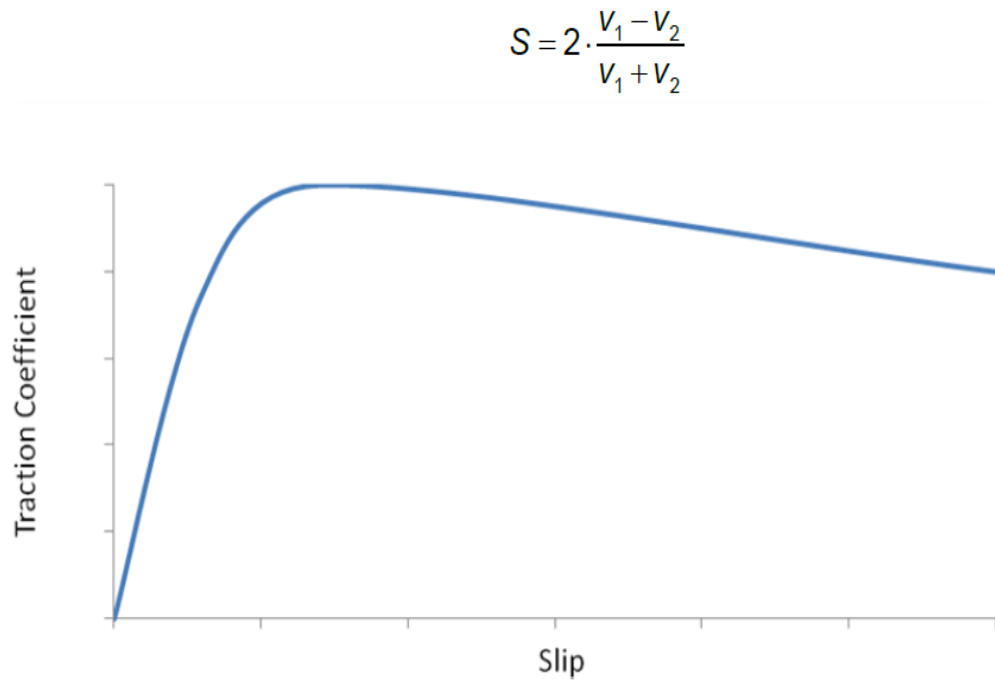


Figure 2.4 General curve of traction coefficient in function of slip [6]

Pure rolling takes place in the contact area when the surface velocity of the two bodies is equal. In the case of two equal cylinders in contact, they must have the same rotational speed. If the circumference velocity is unequal, the rolling motion is accomplished with sliding.

### Slip-rolling motion

A tribological system under rolling motion and simultaneously solicited with sliding can be denominated as slip-rolling motioned. Sliding occurs when the speeds of the two contacting bodies differ, i.e. the speed vectors at the contacting point are not equal (direction, value). Two different equations exist to express the slip-to-roll ratio:

$$s = \frac{v_1 - v_2}{v_1} * 100\% \quad 2.3$$

$$s = \frac{v_1 - v_2}{v_1 + v_2} * 200\% \quad 2.4$$

Where  $v_1$  and  $v_2$  are the speeds of the contacting bodies. The first expression (Eq. 2.3) is widely used and facilitates the understanding of the movement. The main specimen fig 2.5., the one of interest, is noted one, and the sign of its speed is always positive. The counter body (or counterpart) is indexed as two, and the sign of its speed is also positive to fulfill the basics of rolling. If this sign is positive then the counter body rolls in the opposite direction as the main body. And the speed vectors point in the

same direction at the contacting point. The condition of rolling motion is satisfied. The slip amount or slide-to-roll ratio then depends on the value of the speed of the counter body. Explicitly, for a higher speed of the counter body ( $v_2 > v_1$ ), the slip ratio will be negative and in the case of a lower speed ( $v_2 < v_1$ ), it will be positive. With a positive slip ratio, the resulting friction force  $F_R$  acts on the main specimen opposite to the rolling direction. [5]

For a negative sign of the counter body, it has the same motion of the main body and the resulting speed vector has an opposite direction at the contact point. However in this case, the slip is so high that it does not meet the fundamentals of rolling. [5]

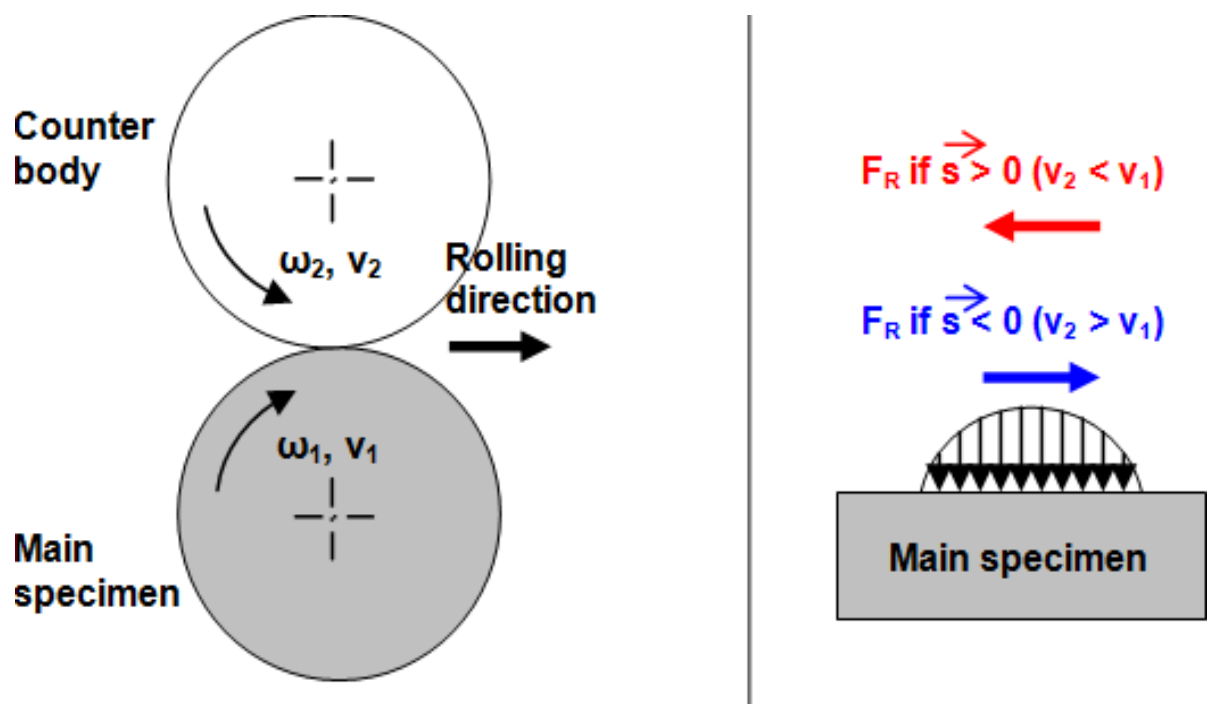


Figure 2.5 Slip-rolling motions [5]

## 2.3. Adhesion basics

### 2.3.1. Coefficient of adhesion

Adhesion is a fundamental feature of all railways systems that have rolling contact between wheel and rail. Some basics of wheel rail contact are given briefly in [10]. Motion of railway wheel is shown in the figure 2.6 .The motion of contact is taken to be at rest and the motion of the rail and wheel is relative.

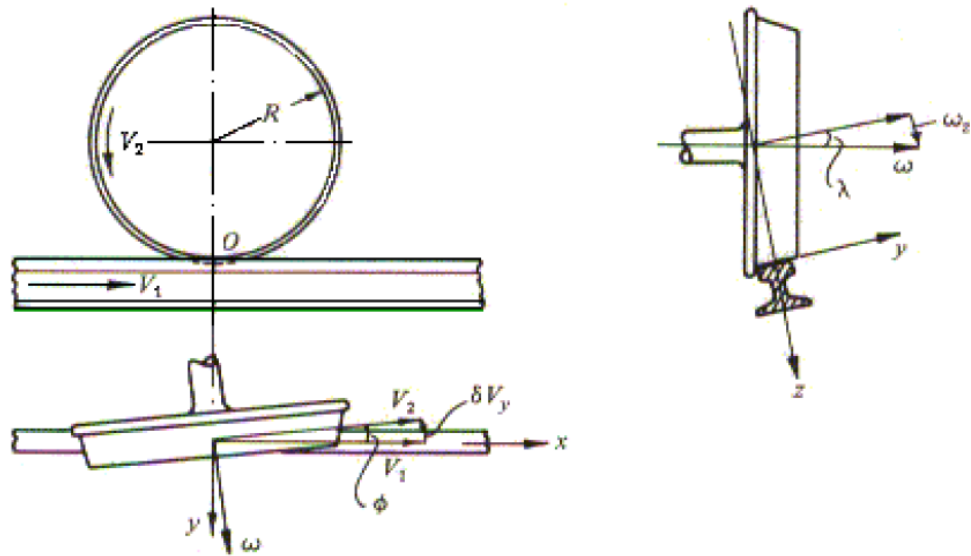


Fig 2.6 Creep motion of railway wheel [10]

If the tangential velocity, relative to the train, of the wheel in the contact region ( $V_2$ ) is not equal to the velocity of the rail relative to the train ( $V_1$ ) then the difference in the velocities causes slip in the contact in the direction of motion. In general, there is also a component of spin So that slip within the contact patch is not always parallel with the motion caused by the conicity of the rail/wheel contact and in curving, the angle of attack. Free rolling is a term used to describe motion without sliding or spin. When free rolling occurs, the traction force is zero and adhesion is zero too. In a motion where traction force is non-zero we use the term tractive rolling [10].

The force that is responsible for traction, steering and braking of railway vehicle is transmitted through a very small wheel-rail contact patch. The geometry of that contact is very complex because of the profiles, angles and displacements involved [10].

Adhesion is the term that describes special condition of friction between wheel and rail when there is both rolling and sliding present. It is measure of the 'grip' available between wheel and rail, i.e. a measure of slipperiness. The coefficient of adhesion (coefficient of traction)  $\mu$  is the ratio between the traction force that can be applied tangentially to the wheel at the wheel/rail interface and the normal load ( $\mu=F/N$ ). The value of adhesion is generally expressed as a decimal fraction or as a percentage. It is a function of creep and in the most papers it is used as the basic curve to estimate changes of adhesion due to various factors.

Wheel and rail are elastic bodies, which deform under rolling contact, so some of the contacting points may slip and others may stick. When free rolling, the whole of the contact is sticking ; with tractive rolling, on the other hand, the contact patch is divided in to 'stick' regions and 'slip' regions, and as the traction increases less and less of the contact patch sticks. When the whole of the contact patch is slipping, the adhesion coefficient is maximum, and equal to the friction coefficient. This is illustrated in fig 2.7

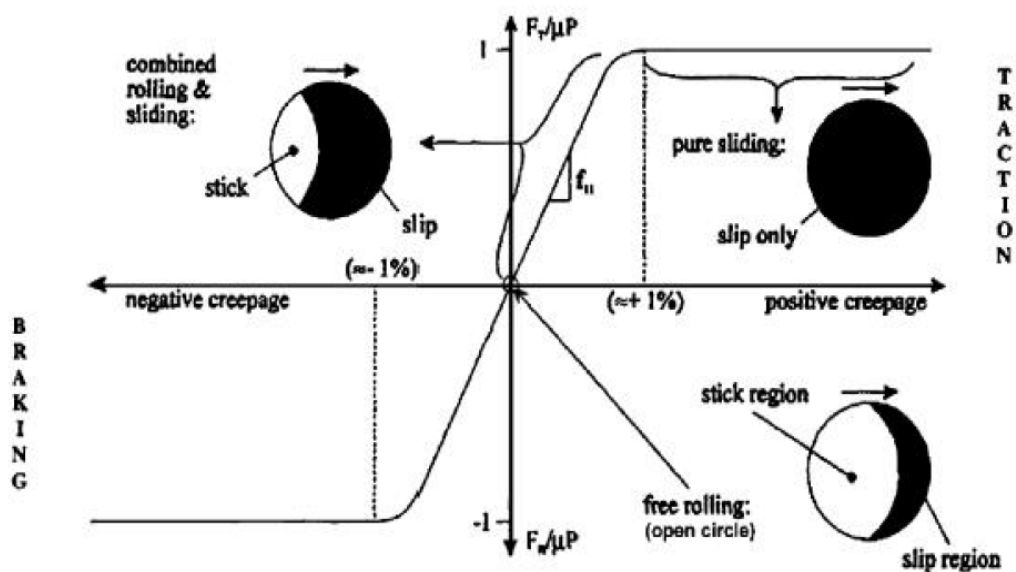


Fig 2.7 Schematic depiction of full traction curve with stick and slip regions [10]

The product of the coefficient of adhesion ( $\mu$ ) and the acceleration due to gravity ( $g$ ) is approximately the maximum possible rate of deceleration of the train. For example, for braking a train we need a braking rate of 9%, i.e. an adhesion level of 9% (or 0.09). For starting a train a higher coefficient of adhesion is needed, between 15% (0.15) and 25% (0.25).

For rail operation a high coefficient of adhesion is preferable. In laboratory conditions, with clean and dry steel on steel, this coefficient can go as high as 0.6(60%). On track this value is seldom obtained. In dry weather, with clean uncontaminated rails, the adhesion level is typically 0.4-0.5 and this is considered high. Average adhesion is about 0.3 and in wet conditions it may be between 0.1-0.2. These values are sufficient for train braking. From the measurements done by British Railway research Tribometer train it can be seen that for most of the time the available adhesion levels are sufficient for correct performance of trains, both for traction and for braking. Very low levels of adhesion (below 0.02) and also very high levels (above 0.35) are rare. Some researchers have found it useful to clarify low adhesion as follows [10]

- High ( $\mu > 15\%$ ) – clean rails wet or dry
- Medium ( $10\% < \mu < 15\%$ ) – damp rails with some contamination
- Normal low ( $5\% < \mu < 9\%$ ) – typical Autumn mornings due to dew/dampness often combined with light overnight rust
- Exceptionally low ( $2\% < \mu < 4\%$ ) – severe rail contamination often due to leaves but sometimes other pollution.

Adhesion varies all the time and the value on any given date and time, even on any given date and time, even on particular track, cannot be predicted with certainty. Change of  $\mu$  can be rapid and also short-lived, and values can differ from position to position along the route. The reason for this variation is that rails are often contaminated and  $\mu$  depends on the type and degree of contamination. Environmental conditions such as temperature and humidity have a great influence on adhesion.

### **2.3.2. Wheel–rail contact conditions**

Unlike road vehicles, such as the automobile, railway vehicles have some unique behaviors and properties, such as hunting motion, self-steering capability, and lateral dynamics. These unique features originate from the wheel–rail guidance system depending on wheel and rail geometry. First, the rail has a specific profile [1,2,3], governed by rules, and is mounted at a small inwards inclination (1:30 in Sweden) (indicated by no. 3 in Fig. 2.8) for better fit to the wheel profile and better load transfer to the sleepers and ballast. Second, the wheel is of a special design, including a wheel tread (where contact point 1 is located on the wheel in Fig. 2.8) and wheel flange (where contact point 2 is located on the wheel in Fig. 2.8). Moreover, the wheel

profiles are usually conical (indicated by no. 4 in Fig. 2.8), leading to the difference in rolling radius in a curve for the two wheels in the same wheel set. Compared with tire–road interaction, the wheel–rail contact is very small at approximately  $1 \text{ cm}^2$  [5]. As a result, the heavy axle load is transferred through a small patch generating high contact pressure.

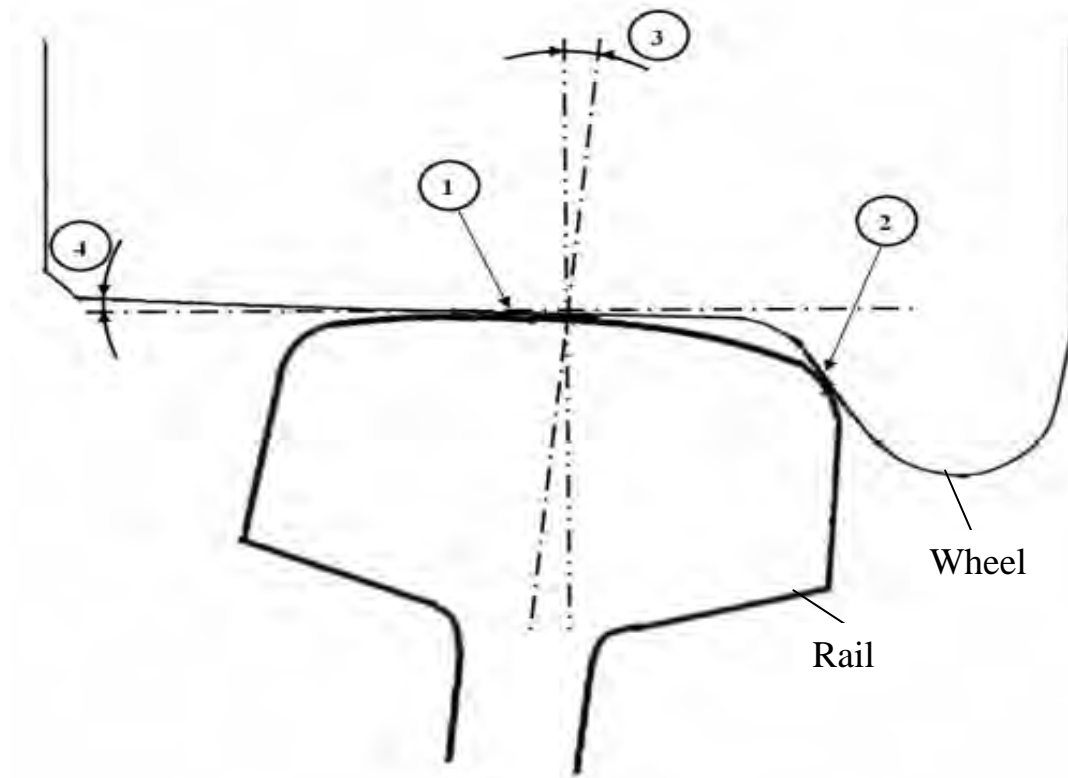


Figure 2.8 Schematic of two types of wheel–rail contact: 1. wheel tread–railhead contact and 2. Wheel flange–rail gauge contact; 3. rail inclination; 4. conical wheel profile [1, 2]

The two basic types of wheel–rail contact differ in many respects. Yi Zhu [1, 2] presented the operating conditions in a wheel tread–railhead contact and a wheel flange–The wheel–rail contact is a rolling–sliding contact. It is easy to imagine wheels rolling on tracks. On the other hand, wheels will also spin if the tracks are very slippery, for example, if there is ice on the track, in what is known as sliding motion. The combination of the two motions is called rolling–sliding contact. The difference between the circumferential velocity of a driven wheel and the translational velocity of the wheel over the track is usually a non-zero value, which is known as sliding velocity. The ratio of sliding velocity to rolling velocity is called slip or creep [1, 2],

which is the main source of creep force. In this thesis, we relate creep to a positive value assuming the vehicle is braking.

Due to the above-mentioned factors, the wheel–rail contact area changes when running under different conditions. Generally, when the vehicle is running on a straight track, the contact area is usually between the wheel tread and railhead, as shown by contact point 1 in Fig. 2.8. When the vehicle is running on a curve, the contact area moves to between the wheel flange and rail gauge, as shown by contact point 2 in Fig. 2.8, or both of contact point 1 and 2. However, in real operation, the wheel rail contact varies constantly in terms of area and type, even starting from the same profile. In railway maintenance, wheels need to be changed and rails need to be re-ground after a certain time, depending on the contact conditions and wear.

## 2.4. Causes of low adhesion

The main reason for low adhesion is railhead contamination. Low adhesion can come from [3,10,34]:

- Light rain or drizzle, dew, snow, ice on the rail, general humidity due to humidity,
- Crashed damp leaves,
- Damp rust,
- Solid particles like rust or coal dust,
- Spilled diesel fuel, lubricating oil from vehicles, leaking hydraulic fluid from track machines, oil/grease from defective rail mounted flange lubricators
- Chemicals from washing or near industrial sites.
- These conditions are often combined with weather conditions such as air and ground temperature, relative humidity and atmospheric pressure, which are difficult to predict. Measurements of adhesion, however, although not perfect, can give some prediction of low adhesion sites.

## 2.5. Contamination of contact surface

As a rolling–sliding contact, a wheel–rail contact is similar to a rolling ball bearing or gears [15, 16], though these are mostly closed systems with comparatively good

lubricating conditions. The wheel–rail contact is an open system, which makes it extremely difficult to transfer knowledge from other well-studied but closed systems. For example, the friction coefficient on the railhead is high on a sunny day but decreases on a rainy day. Even on a sunny day, the friction coefficient can differ depending on the humidity and temperature. In addition, foreign substances, such as sand, dust, leaves, oil or grease, can also be present on the rail. All these factors will influence the friction coefficient, resulting in excessive or insufficient wheel–rail adhesion. Table 2.1 shows the friction coefficient measured using a hand-push tribometer in [2, 12] and even though other current rail adhesion measurement methods as discussed in [13] exist. The friction coefficient varies depending on the conditions, and is generally reduced by water, oil/grease, and wet leaves as discussed in [2, 1, 12, 7, 3, and 14]. Moreover, temperature and humidity can also change the friction coefficient [4, 10]. A typical available friction, i.e., adhesion coefficient, under various conditions is depicted as shown in Table 2.1. Note that sand can increase the adhesion coefficient and moisture can reduce it, compared with outright wet conditions. [1, 2,12]On the other hand, the adhesion coefficient is limited by the coefficient of friction between the wheel and rail despite other factors such as dynamic load variation. For the steel–steel contact under dry, clean conditions, the coefficient of friction is approximately 0.6, which obviously fulfils all adhesion requirements. However, the wheel–rail interface is an open system, meaning that contaminants can enter the contact and affect the friction levels, making the wheel–rail adhesion too high or too low. Table 2.1 shows the friction coefficient measured under different conditions [1].

Table2.1. Friction coefficients measured on metro lines using a hand-pushed tribometer [1].

Conditions	Temperature (°C)	Friction coefficient
Sunshine, dry rail	19	0.6–0.7
Recent rain on rail	5	0.2–0.3
A lot of grease on rail	8	0.05–0.1
Damp leaf film on rail	8	0.05–0.1

Table 2.2 Examples of wheel–rail adhesion coefficients discussed in [2, 12]

Rail conditions	Adhesion coefficient	Rail conditions	Adhesion coefficient
Dry and clean	0.25–0.3	Moisture	0.09–0.15
Dry with sand	0.25–0.33	Light snow	0.10
Wet and clean	0.18–0.20	Light snow with sand	0.15
Wet with sand	0.22–0.25	Wet leaves	0.07
Greasy	0.15–0.18		

In the context of the railway track, contamination refers to any material that is present on the rail and becomes entrained in the wheel–rail contact. The contamination can be divided into solid contamination, such as sand, dust, leaves, and debris, and liquid contamination, such as water, oil or grease as discussed in [10]. Of these contaminants, sand is usually used to increase adhesion and remove surface layer contamination, since modern power cars and locomotives require a higher friction coefficient on the railhead. Liquid contaminants and leaves can reduce adhesion, especially when the rolling speed is increasing. Dust or debris could reduce the adhesion by mixing with liquids [2, 12]. As a result, the dominant problem is too low adhesion in the wheel tread–railhead contact. This thesis focuses mainly on low adhesion in the wheel–rail contact caused by water, oil, and the leaf-formed blackish layer.

Since the wheel–rail system is an open system, any contaminants present between the wheel and rail affect the adhesion. Contaminants such as water, iron oxide, and leaves, which are unintentionally present on the rail [1] (“natural third-body materials”), should be distinguished from flange lubricants and friction modifiers deliberately applied to the rail or wheel (“artificial third-body materials”). All of the above can be termed “third-body materials” [1] that forms a third body between the bulk materials of the wheel and rail. Third bodies, such as iron oxide or leaves, sometimes become chemically bonded to the surfaces of the bulk materials. Therefore, in practice, the actual materials forming the wheel–rail contact can differ chemically from the wheel and rail steels forming the actual wheel and rail, as shown in Figure 2.9.

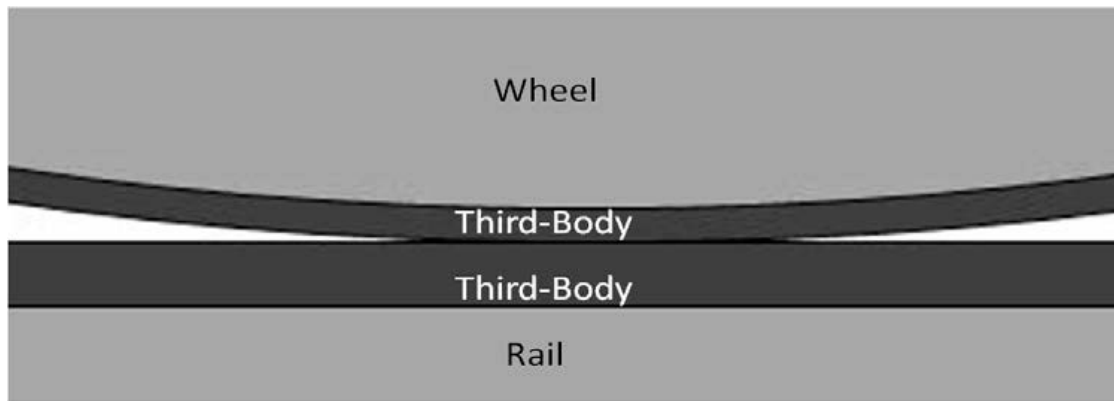


Figure 2.9 the third-body layer between the bulk materials in the wheel–rail contact [1]

Liquid contaminants, such as water and oil, are often used as lubricants in certain industrial applications. Lubricants significantly affect wear and friction and will usually improve the lifetime performance and reliability of a machine. Richard Stribeck was a German mechanical engineer at the TU Dresden. He observed that for low velocities, the friction force is decreasing continuously with increasing velocities. This phenomenon of a decreasing friction at low, increasing velocities is called the Stribeck friction or effect. The effect of contact speed on the friction coefficient of a lubricant can be described by a so-called Stribeck curve as shown in figure 2.10. Two disc test machines are often used to determine these curves for different lubricants by determining the traction forces that occur for rotational speeds at a certain normal load. Stribeck studied the effects of lubricants in various lubrication regimes as a function of relative surface velocity (see Fig. 2.10). In the boundary lubrication regime (BL), the velocity is relatively low. The film build-up is negligible and the load is borne mainly by asperities. The main function of the lubricant is to reduce the adhesion component (i.e., atomic forces) of friction. In the full film lubrication regime (FL), the velocity is high and the two surfaces are fully separated by lubricant; the friction depends mainly on the shear stress in the lubricant. The region between BL and FL is known as the mixed lubrication regime (ML), in which part of the load is borne by asperities and part by lubricant. The friction of ML ranges between those of BL and FL. Elastohydrodynamic lubrication occurs when the surface deformation helps to form a film. The application of the lubrication regime concept to wheel–rail adhesion under water- and oil-lubricated conditions could yield a better understanding of the adhesion-reduction mechanism. Furthermore, since field tests or full-scale tests are usually expensive to run, it is crucial to find a connection between scaled lab tests and the real

situation. The Stribeck curve and calculated film thickness parameters could be used to compare scaled tests and the real situation in terms of lubrication regimes, which is very important for selecting parameters and making comparisons in scaled tests [1, 2, 9 and 17].

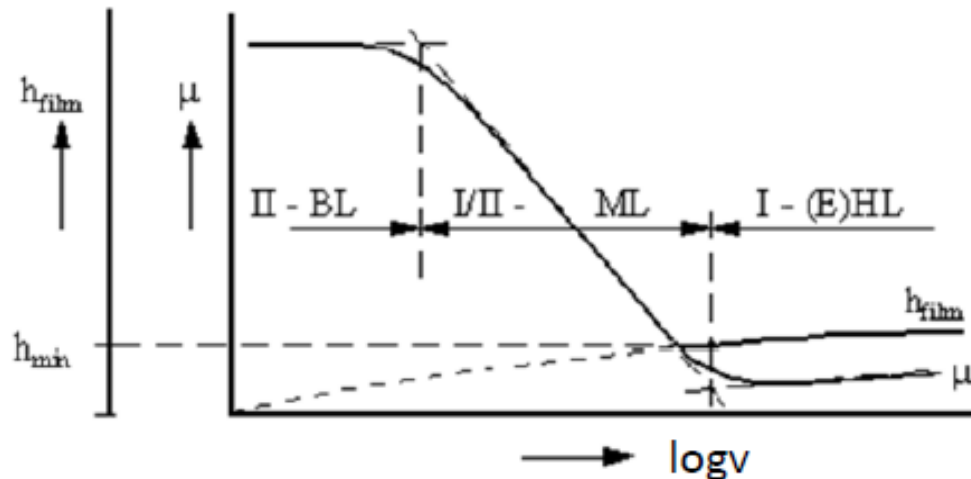


Figure 2.10. Stribeck curve [1, 2, 17]

### 2.5.1. Mechanism of adhesion loss due to water and oil

Water and oil are very common contaminants, both of which are known to reduce adhesion between the wheel and rail. Oil can reduce the adhesion coefficient much more than water can when the speed is increased within a low speed range. The fluid load capacity is inversely proportional to the adhesion coefficient. The load carried by water is much less than that carried by oil, though both cases are in the mixed lubrication regime. This is because that the viscosity of water is only 0.1% of that of oil. According to the investigations so far water causes only a very small reduction in the adhesion coefficient on stainless steels, but a small amount of water mixed with oil or wear debris can reduce the adhesion substantially [1, 2, 17].

Rail surface contamination is the primary reason for loss of adhesion. Fallen leaves (especially leaves with oil [e.g., pine and cedar leaves]); a little water, frost, or light drizzle; and morning hours produce the worst conditions for maintenance of adhesion. Rust, dry dirt, and other dry contaminants on top of the rail, by themselves, do not affect adhesion much; however, the presence of small amounts of water and oil results

in the formation of a thin slurry or paste that reduces adhesion. Heavy rains do not reduce adhesion as much because they tend to wash the rail and remove the slurry.

Poor adhesion arises to cause significant operating difficulties because of the sensitivity of the adhesion coefficient to rail head contamination. Even when the running band (where contact takes place) is clean and shiny, it contains some kind of contamination. Past research shows that very high levels of adhesion can be found only under laboratory conditions up to 60% (0.6). Even a very small amount of contaminant can significantly reduce adhesion. The highest level of adhesion on track measured with tibometer train was variation and unpredictability of adhesion value is its dependence on weather conditions, such as temperature and humidity. These factors combined with various kinds of debris can lower adhesion to 0.02.

## **Water**

The most important cause of low adhesion is water and this has been widely discussed in [10,19]. The presence of water can be through heavy/ light rain, snow, drizzle, dew, or misty conditions. Combined effects of temperature and humidity are another aspect of this problem. When there is small amounts of water, or when rails are drying after rain, these are the moments when low adhesion conditions are most likely to arise. This can happen in very light drizzle, during mist or dewy morning. The coefficient of adhesion may drop to 0.1. If water is combined with contaminants, like overnight rust or crushed leaves, adhesion condition may become exceptionally low, down to 0.05. Fortunately, often these exceptionally low adhesion don't last since the contaminant film is quickly destroyed by passing wheels.

Rain can reduce adhesion almost instantly, usually to a level of 0.2 or 0.25. This is not below the level required for normal train operation. The influence of rain is the main reason why the average adhesion levels are lower in autumn than in summer. Another problem with rain is that it can affect significant lengths of track.

On the other hand, a heavy rain often increases adhesion because it washes contaminants off the rails and also keeps fallen leaves on the ground and prevents them from blowing onto the railhead by the turbulence of passing trains.

Humidity is also associated with low adhesion. Water molecules are constantly absorbed from the humid atmosphere. More water is absorbed as the humidity increases.

The water temperature has a clear influence on the traction coefficient, which decreases with a decrease in water temperature [10]. This phenomenon is related to water viscosity, which decreases as temperature rises. Water film is thinner at higher temperatures and is easily broken by asperities of wheel and rail. Accordingly, the coefficient increases figure (2.11) shows enlarged contact of the two surfaces.

Generally, water can be considered as a weak lubricant, which is enough to reduce adhesion, but because of the small size of the water molecule it cannot form protective films as oil can. Water also triggers surface oxidation of the rail steel and forms rust.

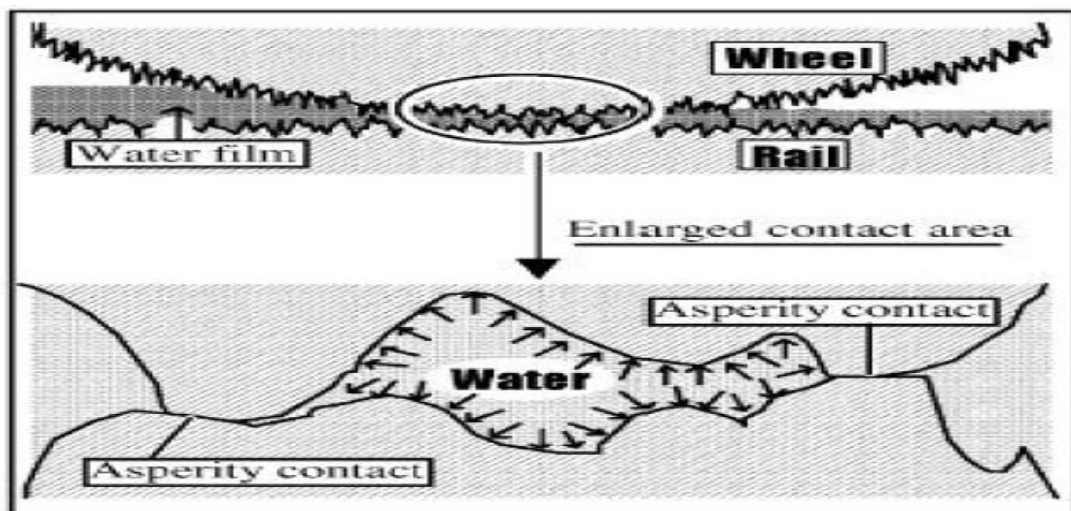


Fig 2.11 Concept of partially lubricated contact [10]

## Oily Materials

After water, oil is the most common rail contaminant. Oil can come onto the rail head Spillage from track machines (hydraulic oil), badly adjusted trackside flange lubricators (grease), near airports (aviation fuel –kerosene), but this is rare and is unlikely to produce serious adhesion problems. Specific locations may become particularly affected, such as where locomotives regularly stands at a signal, or as an extreme case, spillage from a vehicle in motion. However, under the action of passing wheels thin film of oil can be transferred along the track and increase the area affected. Even minute quantities of film will lower adhesion. Such thin oil films, under the extreme pressure of passing wheels and the action of sunlight, humidity and temperature, rapidly oxide and bond strongly to the rail head. However, track circuits will not be isolated because, due to asperities of surface roughness, metal to metal contact is not completely eliminated [10, 34].

## Leaves

In addition, rail services worldwide are disrupted by fallen leaves. In autumn, leaves fall on the rail lines, forming a blackish layer when they are crushed by passing wheels, resulting in serious adhesion loss. These leaves do not have to fall precisely on the tracks. The turbulence of each passing train stirs up dead leaves that were previously on the track ballast by its slipstream swirling around the vehicle and getting crushed by passing wheels. The crushed leaves eventually form a hard, slippery, blackish layer that strongly adheres to the rail surface and is very difficult and expensive to remove. This layer gives a friction coefficient of 0.1, or of 0.05 or even less when combined with a small amount of precipitation[35]. Some lab tests simulating the ‘leaves on the line’ problem have been conducted, indicating that a chemical reaction occurs on the rail surface resulting in low adhesion. However, the exact mechanism of the layer formation remains unknown, since it is very difficult to run tests that exactly reproduce the real situation. Furthermore, leaves cannot be treated as lubricants, so classical tribology theory cannot be applied [8, 10, 35,36]. In examining various contaminants, the term ‘lubricant’ refers to water and oil/grease in the following section.

### 2.5.2. How do leaves on rails reduce the adhesion coefficient?

According to Yi Zhu [1,2] leaf contamination on railhead surfaces by comparing different rail samples cut on five occasions over a year. Surface chemistry results indicate that the tarnished rail sample taken in October differs greatly in elemental content and depth profile from the samples taken on other occasions. The tarnished layer is much softer than the non-tarnished layer of the same running band. These facts indicate that the tarnished layer results from a chemical reaction between the leaves and bulk materials, and that the chemical reaction occurs from the surface to a depth of several microns. As described by Zhu the oxide coating structure can be divided into three sub-layers. The superficial sub-layer is the friction-reducing layer that plays the key role in reducing the friction of steel. As was performed an additional study by measuring the thickness of the friction-reducing layer, and obtained very interesting results. The measured friction coefficient is inversely proportional to the thickness of the friction-reducing oxide layer, i.e., the greater the thickness, the lower the friction coefficient. The tarnished-layer sample has the thickest friction-reducing oxide layer

of all the samples. Moreover, two other samples taken in October, one with leaf residue and the other with no visible contamination, also have much thicker friction-reducing oxide layers than do samples taken on other occasions, though these oxide layers are much thinner than the tarnished layer. This fact indicates that all three samples were contaminated with leaves, though they differed in appearance, the appearance being related to the degree of leaf contamination.

## **Rust**

On the well used mainline tracks contact takes place along a clean and shiny wear (or 'running') band between heavily rusted shoulders. Although this wear band appears clean, it will inevitably have a light contacting of iron oxide and hydrated iron oxide (rust). These sub-micron sized particles can be seen under the microscope.

Rust has an ability to absorb oils that drip onto the rail surface. The most significant effect of rust on adhesion is when it is combined with small amount of water. Then thin oxide film form which protects the surface from metal to metal contact. However rust is an undesirable product which reduces the adhesion level, especially when combined with other contaminants [3, 10, and 35].

### **2.6. Twin-disc Test apparatus description**

There are two main types of laboratory test rigs detailed in [18]; the full size wheel-on-rail test rig and twin disc machines as described below. In addition there are a number of similar devices that may be useful for simulating low adhesion conditions:

- a) Independently motor controlled twin disc machine (Sheffield University)
- b) 1/3 scale twin disc machine (Manchester Metropolitan University)
- c) 1/5 scale roller rig (Manchester Metropolitan University)
- d) Pin-on-disc machine.

The twin disc machine which is described by Kenza Ikoubel [14] shown in figure 2.12 is connected to a computer where the "tribosoft" software can be started. The software consists of two windows (Measurement and Setup). The setup window allows the change of the test parameters. The diameter of the test samples, the suited load, the desired velocity in rpm or m/s are inserted. When the rolling option is selected, both

discs rotate at the same speed. It is possible to select a slip percentage or to enter directly the velocity of the 2<sup>nd</sup> disk if the gliding option is selected. In the case of the research, it is considered that there is no slip. The software makes a file of each current test. Once the modules are confirmed, the machine is set up. The load and wear transducers are tarred. As shown in the figure 2.12, the machine is mainly composed of two servo motors, a torque transducer, load counterweights, a thermocouple, an oil pump and 2 samples rolling against each other. Each of them is driven by a motor [14].

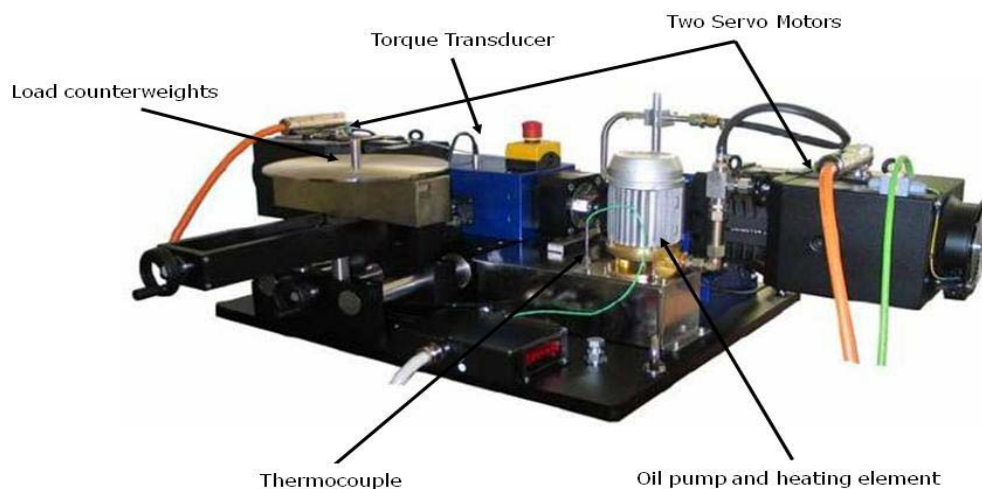


Figure 2.12 UTM 2000 Twin Disc machine [14]

Twin disc machines (such as the Amsler machine shown in Figure 2.13) are commonly used as research tools by industry and academia and provide a laboratory method of testing for friction, wear and lubrication. These machines use discs of approximately 40 mm diameter and can be loaded to reproduce wheel / rail maximum contact pressures. Traction or braking forces can be introduced by using discs with different diameters. [18]

Schematic diagram of the twin disc test machine depicted in [15, 21, 17, and 40] was used to carry out the adhesion testing (shown in Fig.2.1 4). The original development of this machine, and more recent work carried out to add a feedback control system

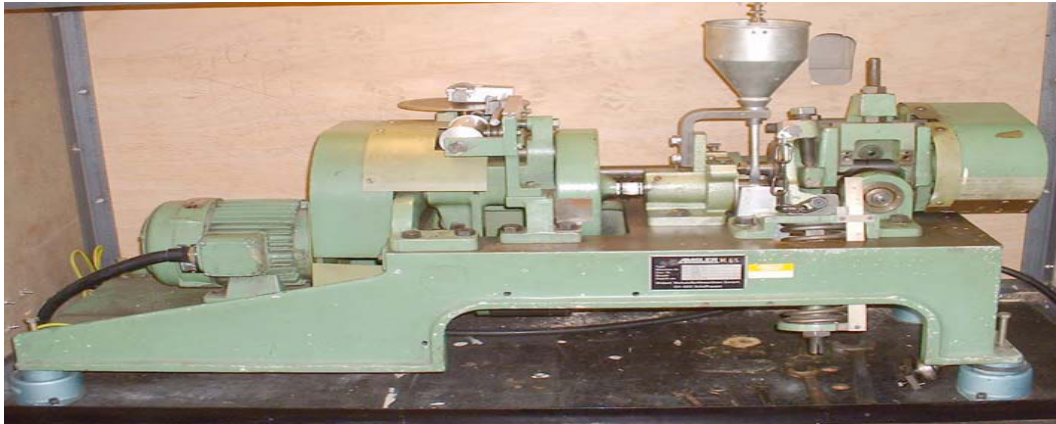


Figure 2.13 Amsler twin disc machine [18]

The test discs are hydraulically loaded together and driven at controlled rotational speed by independent electric motors. Shaft encoders monitor the speeds continuously. A torque transducer is assembled on one of the drive shafts and a load cell is mounted beneath the hydraulic jack. The slip ratio required is achieved by adjustment of the rotational speeds. All data is acquired on a PC which is also used for load and speed control.

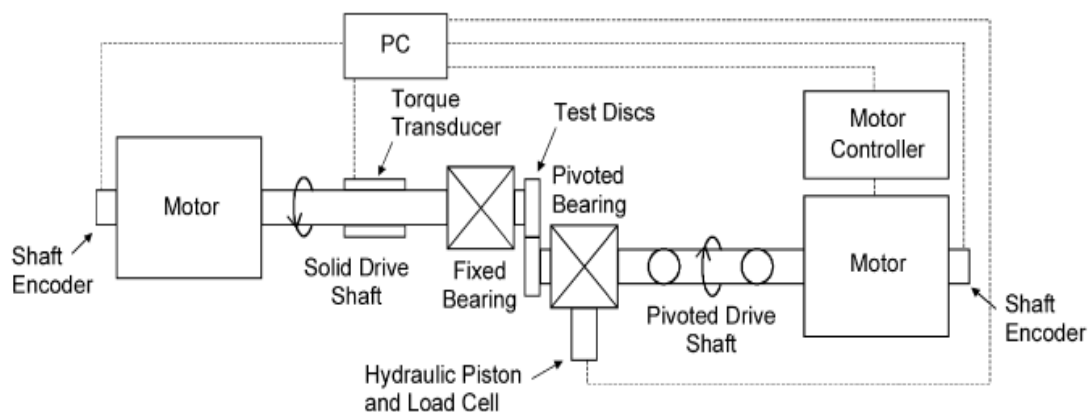


Fig. 2.14 Schematic diagram of the twin disc test machine [3, 10, 20 and 28].

### 2.6.1. Parameters of Lab test with twin disc test machine

As to Oscar Arias-Cuevas, Lewis and Gallardo-Hernandez [3, 19], the slip ratio between the discs was prescribed by setting different rotational speed of the shafts and maintained constant throughout each test with a controller. The slip ratio is defined in Eq.2.1 where  $\omega$  and  $r$  are the rotational speed and rolling radius of the discs, respectively. The adhesion coefficient was calculated with the readings of the torque transducer and the load cell as Eq. 2.2  $T$  and  $F_N$  respectively.

$$Slip = \frac{\omega_{wheel} * r_{wheel} - \omega_{rail} * r_{rail}}{\omega_{wheel} * r_{wheel} + \omega_{rail} * r_{rail}} * 200\% \quad 2.1$$

$$= \frac{V^{rel}}{V^{mean}}$$

Where  $V^{rel}$  relative velocity and  $V^{mean}$  mean velocity of the two discs

$$\mu_{adhesion} = \frac{T}{F_N * r_{rail}} \quad 2.2$$

Where  $\mu_{adhesion}$  adhesion coefficient,  $F_N$  applied force read from force cell and T torque read from torque transducer.

## 2.7. Specimens/Test discs

In many researches, discs to be used during the testing were cut from R8T wheel rims and UIC60 900A rail sections or close to this European standard and machined to a diameter of 47mm with a contact track width of 10 mm. The contact surfaces were ground to a roughness of 1 micron as indicated in [8]. As discussed by [1,2 and 8] rail material designated by UIC 900A in table 2.3 does have a hardness of 300 HB and a minimum tensile strength of 863 N/mm<sup>2</sup>. R7 wheel material is a little softer, in the hardness range of 229–277 HB, with tensile strength in the range of 730–890 N/mm<sup>2</sup>. Wheel specimens were drawn from the wheel rim parallel and as close as possible to the outer surface as shown in the fig. 2.15 left.

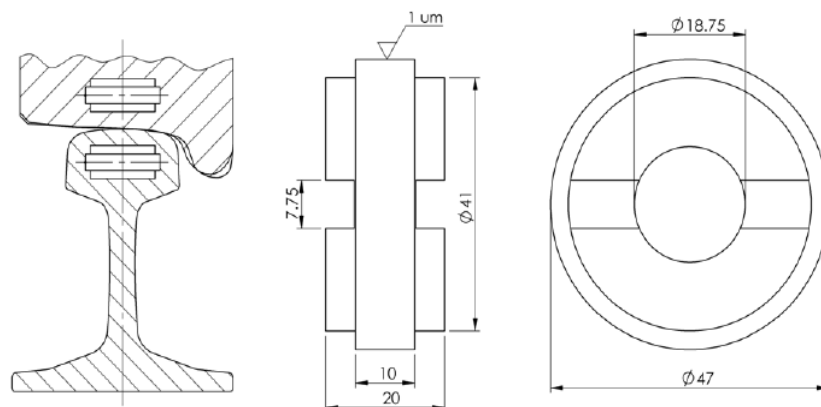


Figure 2.15 Left: Disc specimens are cut from rail and wheel sections. Right: Usual dimensions are 47mm diameter and 10mm track (running) width. [3, 10, 19]

### 2.7.1. Material composition and properties of wheel and rail (specimens)

The specimens consisted of AISI 52100, which is usually used as bearing steel. The material compositions of AISI 52100, wheel, and rail steel are presented in Table 2.3. The hardness of the discs was 300–320 HV, which is very close to that of rail steel.

Table 2.3: Wheel and rail material composition from Yi Zhu [1,2]

Chemical composition (wt %)	C	Si	Mn	P	Ni	Cr
UIC60 900A rail	0.6-0.8	0.15-0.5	0.8-1.3			
R7 wheel	0.52	0.4	0.8	0.035	0.3	0.3
AISI 52100(standard)	0.98-1.1	0.15-0.3	0.25-0.45	$\leq 0.025$		1.3-1.6

Table 2.4: Test Rig Parameters [21]

Description	Value
Lower Disk Radii of curvature (longitudinal, lateral)	0.213 m, 0.300 m
Upper Disk Radii of curvature (longitudinal, lateral)	0.085 m, 0.040 m
Normal Force Range ( $P_0$ )	0 - 2000 N (400N)
Tangential Load Range ( $Q_0$ )	0 - 1000 N
Friction Coefficient ( $\mu$ )	0.45(Dry) 0.15 (Friction Modifier)
Typical Lower Disk Rolling Contact Velocity Range	0 – 1200 RPM / 0 - 26.8 m/s
Disk Material Cast Steel	(0.71%C, 0.46%Si, 0.85%Mn, 0.05%Cr, 0.02% Ni, 0.01% Mo, 0.02% S, 0.02% P)
Yield Strength	420 MPa
Density ( $\rho$ )	7800 kg/m <sup>3</sup>
Poisson's Ratio ( $\nu$ )	0.28

Table 2.5 Mechanical properties of wheel and rail, high carbon steel [22]

Material	Brinell Hardness (HRC)	Shear Yield Strength (MPa)	Ultimate Shear Strength (MPa)	Tensile Yield Strength (MPa)	Ultimate Tensile Strength (MPa)
AISI 1080 (Automation Creations 2005a)	293 (30.5)	330	536	585	965
AISI 1070(Automation); Automation Creations 2005b	212 (16.9)	217	390	385	703

The shear properties presented in table 2.5 were calculated using the work of Guduru et al (1989) as in [22] described in equation (2.1) and (2.2)

$$\sigma_y = 1.77\tau_y \quad 2.1$$

Where  $\sigma_y =$  Yield stress and  $\tau_y =$  Shear yield stress

$$\sigma_{US} = 1.8\tau_{US} \quad 2.2$$

Where  $\sigma_{US} =$  Ultimate tensile strength and

$\tau_{US} =$  Ultimate shear yield strength

The disc specimens of [8] were cut from UIC60 900A rail steel R8T wheel steel sections. They had a diameter of 47mm with a contact width of 10mm as in Figure 2.5.

The contact surfaces were ground to a roughness of 1 micron.



Figure 2.16 Wheel and Rail Disc Specimens taken from wheel and rail [8]

As already seen in the literatures reviewed, the methods, materials and conditions used to quantify the extent of adhesion losses are the basis of acquiring hints what type of parameters should be considered to simulate the contact between the wheel and the rail quality under different contaminants. So far due to the early establishment of railway engineering sector no research has been made in Ethiopia on adhesion loss experimentally thus this thesis is the first in attempting an experimental test with a simplified test machine constructed here.

# CHAPTER THREE: EXPERIMENTAL METHODS, PROCEDURE, AND CONDITIONS

## 3.1. Material

As investigated in different literature, there are several wheel and rail standards but closely similar in their properties. In the entire standards wheel steel material is a little softer than that of the rail differing slightly in the amounts of carbon, silica, and manganese in the steels used.

For Addis Ababa light rail transit (AA LRT), the rail standard used is China National Railways standard of 50 kg/m while the national is 60kg/m. Table 3.1 represents the chemical compositions and table 3.2 .mechanical property of wheel and rail specimens which suits to the standards that of Chinese and UIC900A .

Table 3.1: Material composition of steel wheel and rail steel discs which suit to UIC standard (UIC 900A rail and R7 wheel) and Chinese standard.

<b>Chemical composition (wt %)</b>	<b>C</b>	<b>Si</b>	<b>Mn</b>	<b>P</b>	<b>Ni</b>	<b>Cr</b>
CSN 12071(rail) (AISI/SAE 1070)	0.6-0.7	0.37	0.6-,8			
CSN 12071( wheel) (AISI/SAE 1050)	0.47-.55	0.17-0.37	0.5-0.8	0.035	0.3	0.25

The rail material designated by CSN 12051 in table 3.2 which represents the wheel material does have a hardness of 270-286HB (28-30HRC) and a tensile strength of 700- 850 N/mm<sup>2</sup>. The rail wheel material is a little harder, in the hardness range of 282–330 HB, with tensile strength in the ranging 750–900 N/mm<sup>2</sup>. These specimens prepared for this thesis are types of materials close to wheel/rail material of UIC and Chinese standard. As shown in the table 3.1 the percentage composition of each material is a little bit lower than the percentage composition described in table 2.3 but is within the range assuring nothing is wrong with the selection.

Table 3.2: Mechanical properties of the selected materials for both the wheel and rail disc samples

<b>Material Type</b>	<b>Brinell hardness (HRC)</b>	<b>Yield strength (M Pa)</b>	<b>Tensile strength (M Pa)</b>
CSN 12051(wheel) (AISI/SAE 1050)	<b>270-286</b> <b>(28-30)</b>	<b>460</b>	<b>700-850</b>
CSN 12071( rail) (AISI/SAE 1070)	<b>282-330</b> <b>(30-35)</b>	<b>470</b>	<b>750-900</b>

### 3.2. Feature and Dimension of the test rigs/Specimen

As discussed in most research papers, the maximum outer diameter of the specimens are limited by the maximum diameter that can be extracted from the section of the rail head; the contact width being 10mm to represent the wheel thread and rail top contact. Thus the specimen feature taken from the wheel and rail would have been looked like in fig 2.5/2.6, indeed, in many researches these dimensions are made in use. Unfortunately the unavailability of plasma cutting machine to cut from rim of the wheel has led me finding an alternative way of preparing the specimens with material composition close to the standard wheel rail material, CSN 12051(in Czech standard) for wheel disc and CSN 12071 for rail as depicted in table 3.1. The composition of each material is depicted in the table 3.1 comparing with UIC and Chinese National Railway standard. The dimensions of the twin discs for this thesis are also modified as in figure 3.2., because there is no dimension limitation as it would have been taken from the rail section. As the name implies, Twin Discs, both the wheel disc and the rail disc have the same dimensions and shape. The effective diameter of both rigs are made 100 mm while the contact width remained to be 10 mm to represent the contact area of the wheel thread and rail top of the real contact .

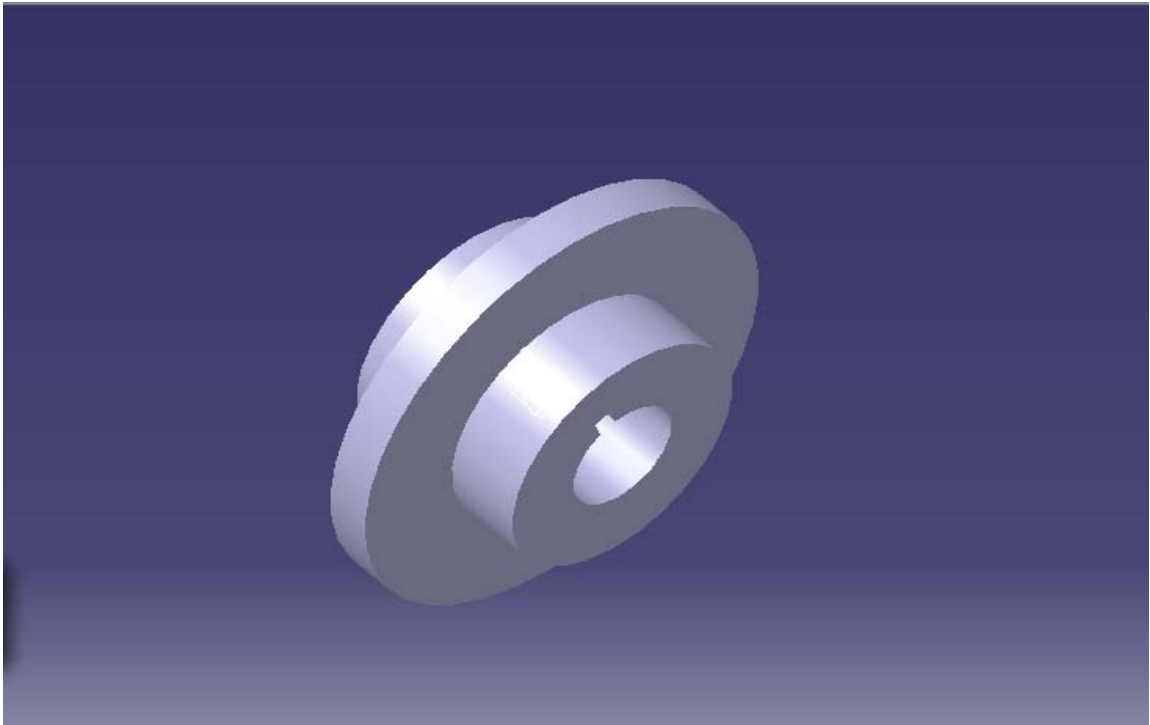


Figure 3.1 Feature of the test rig in CATIA V5.

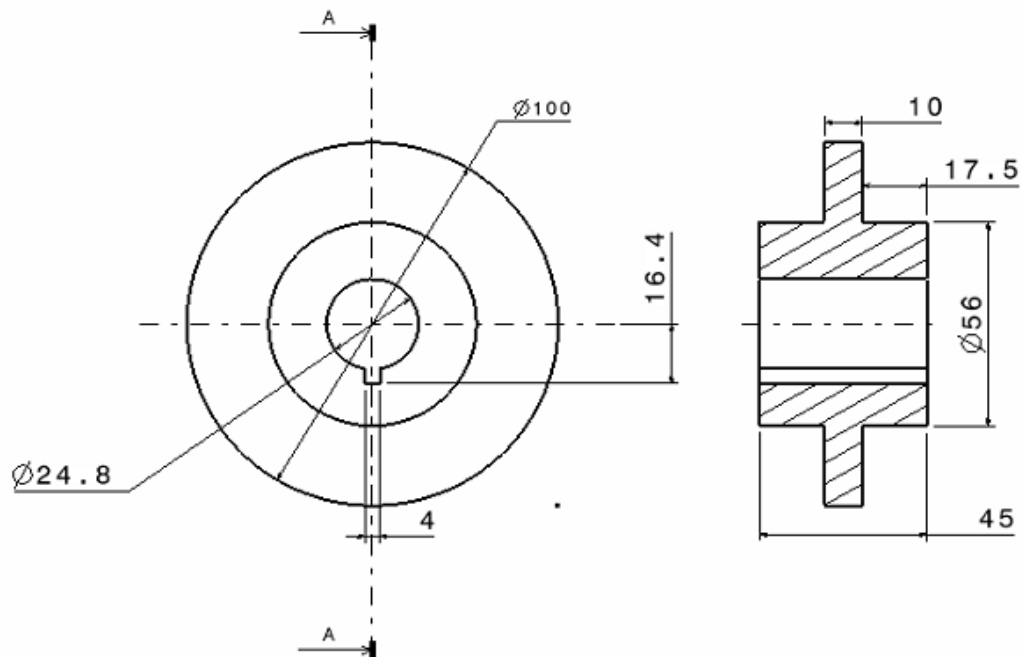


Figure 3.2 Dimension of the Test rigs



Figure3.3 Photograph of the test discs that are manufactured

### 3.3. Method and Test Description

The twin disc test approach has been used to produce creep curves for a number of different contact conditions. This method, while not having the scale or geometry of the actual contact, provides a good simulation of the rolling-sliding motion and allows close control of operating parameters not available in more complex test methods. Tests have been carried out over a range of preset slip values with in Eq. 3.3 and creep curves have been generated.

#### 3.3.1 Test set-up and Conditions

The adhesion test was carried out under the conditions of different wheel/rail contacts, such as various speeds of the wheel disc while rail disc made constant throughout the tests, contact load of 400N, and dry and contamination situation (water, mud, leaves, oil and grease.). In order to generate slip, we adapt a method by presetting the two motors' speeds which the rotation speed of the part of the braking motor i.e. the rail disc motor made 400rpm throughout while wheel disc motor speeds are varied from 400rpm to 442rpm so at create slip values of 0 to 10% calculated from Eq.2.1. In this process, the torques induced were calculated as in Eq. 3.1 from the parameters such as armature voltage and armature current read form the voltmeter and ammeter which are connected to the wheel disc motor .This motor is a DC shunt type which is used for lab test because its speed torque characteristic is known to be good. So that all data: speed,

voltage and current were taken from this special type motor to calculate the torques to corresponding slips of 0 to 10% at each contaminant application.

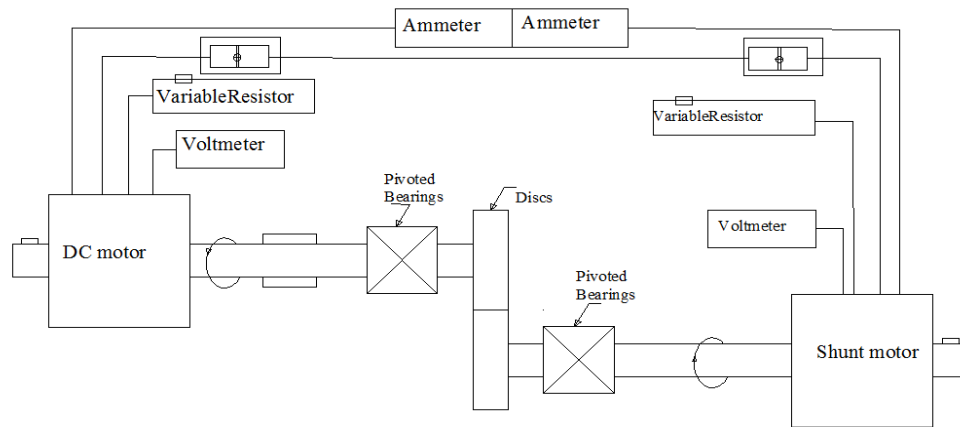


Figure 3.4 Schematic representation of the setup

The set-up of the test apparatus as illustrated in figure 3.4 and 3.5 includes vacuum cleaner to prevent the environmental chamber clogging. For determination of adhesion coefficients at each application of the contaminant, the friction characteristics of contact bodies should be considered by taking into account the roll mode with a slip. For this purpose, a friction machine was used with a set-up as in figure 3.4.



Figure 3.5 Photograph of the set-up

The test settings for this test case were as follows:

- (a) Normal contact load of 400 N due to the applied load of 120N through the T-bolt;
- (b) Different steel materials to represent wheel and rail of rail vehicle as described in section 3.1;
- (c) Diameter of each wheel roller is 100mm as in figure 3.2;
- (d) The wheel disc is a little softer than the rail disc to represent the real situation as depicted in table 3.2;
- (e) Angular speeds of the wheel roller were preset 400 to 442 rpm so as to create slip value/relative slips of 0 to 10%;
- (f) Torques due to the influences of the contaminants could have been read directly from a torque transducers had it been fitted on the shaft of the motor but it was calculated from the induced armature volts currents and the corresponding, speeds as in equation 3.1.

$$T_i = \frac{60(E_a I_a)_i}{2\pi N_i} \quad \text{Eq.3.1}$$

$$= \frac{9.55(E_a I_a)_i}{N_i}$$

Where  $T_i$ ,  $E_a$ ,  $I_a$  and  $N_i$  are Torques armature voltage, armature current and rotational speeds from 0 to 10% slips at each contaminant application Armature voltage, armature current and rotational speeds respectively.

- (g) The corresponding adhesion coefficients are calculated as in Eq3.2.

$$\mu_i = \frac{T_i}{T_{const}} \quad \text{Eq.3.2}$$

Where  $\mu_i$  and  $T_{const}$  are adhesion coefficients at each slip values and constant torque due to the applied load respectively.

- (g) Preset slip values are calculated with formula [Eq. 3.3] below.

$$Slip = \frac{\omega_{wheel} * r_{wheel} - \omega_{rail} * r_{rail}}{\omega_{wheel} * r_{wheel} + \omega_{rail} * r_{rail}} * 200\% \quad \text{Eq.3.3}$$

### 3.3.2. Tested contaminants

As shown in figure 3.6, five contaminants were considered to simulate adhesion conditions of wheel rail contact with twin disc test machine. These were mainly chosen because they are intentionally or unintentionally inevitable to occur as contaminants in the wheel-rail contact.

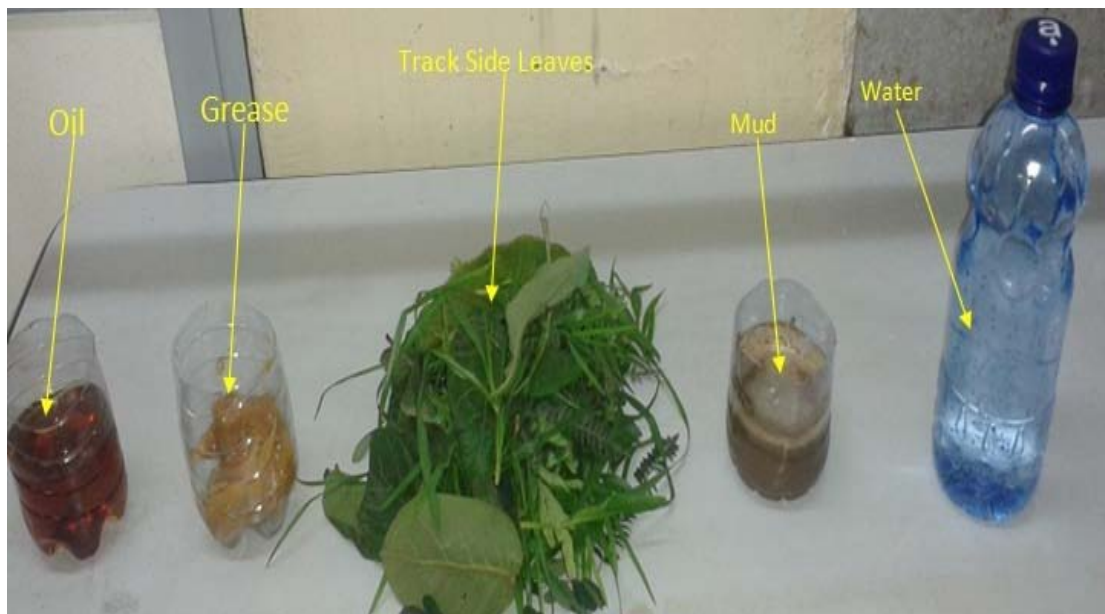


Figure 3.6 Photographs of the contaminants in to consideration for adhesion testing

### 3.4. Test Procedure

The tests were carried out using the wheel disc as the driving disc and the rail disc as the braking disc. The rail disc rotational speed of 400rpm was used and a contact force of 400N. The tests were carried out at slips of 0,0,25, 0.5%, 1%, 2%, 3% up to 10% representing values typical of wheel tread and rail head contacts. For tests with water and oil the supply of liquid was started prior to loading the discs together then the whole test was run lubricated. The mud test was run in a similar fashion. For tests with leaves, the discs were run dry until the traction coefficient stabilized and then the leaves were added. Suction was applied to draw the leaves through the contact and prevent them clogging the environment chamber. A chute was used to apply to a twin disc contact. Leaves were fed down the chute at a rate sufficient to ensure a continuous supply to the contact. Lastly of course the oil and grease test respectively.

### **I. Dry test**

Tests were initially run dry with no contamination i.e. dry test. This test was performed from zero slip to ten percent. Test one of the dry test, at 0% slip, the rotational speed of each motor was adjusted to 400rpm prior to loading each disks together. Then the upper disk was lowered by releasing the load arm lock from its rest pivot and made to meet to the lower disk. Insuring the two discs are perfectly aligned at their 10mm contact width and seen run smooth, a force of 120 N is applied through T- bolt compressing the spring 6mm through the guide and the required force of 400N at the disks contact creating constant torque of 6Nm. The disks were run until stable and data were collected i.e. speed by speed sensor (speedometer), armature voltage from the voltmeter and current from ammeter. In the same manner the corresponding data were collected for the rest of slip values of the dry test.

### **II. Water and mud test**

Next to dry test the test was carried with water. Water was poured by a plastic bottle enough to keep the discs completely wetted for each slip value and data were collected as were done in dry test. After finalizing the test with water, the test was performed with mud the same fashion as water was poured at the top of rail disk and data were collected as the same scenario.

### **III. Leaves test**

The leaves used in this experiment were taken from main road sides, 5 kilo to Meskel Square which also likely to exist along the track sides of railways in the future. Once they were picked up, they were rinsed in water to remove dust particles and made ready for use.

Prior to leaves testing, the disks and surrounding were cleaned well so as to avoid the effects of previous contaminants other than the leaves. As was done in the preceding tests starting with zero slip the test were strictly done for all of the slip values. Since the cylindrical disks were used in the experiment, a line contact of 10mm width was present. A load of 400N was applied on the disks as in the preceding test. Prior to application, the leaves were cut into pieces smaller than the disk contact width to ease

their entrapment into the disks interface. They were manually fed through a chute to the disks interface as in figure 3.7 below and being drawn through by a suction system, vacuum cleaner located on the other side of the disks as depicted in Figure 3.5.

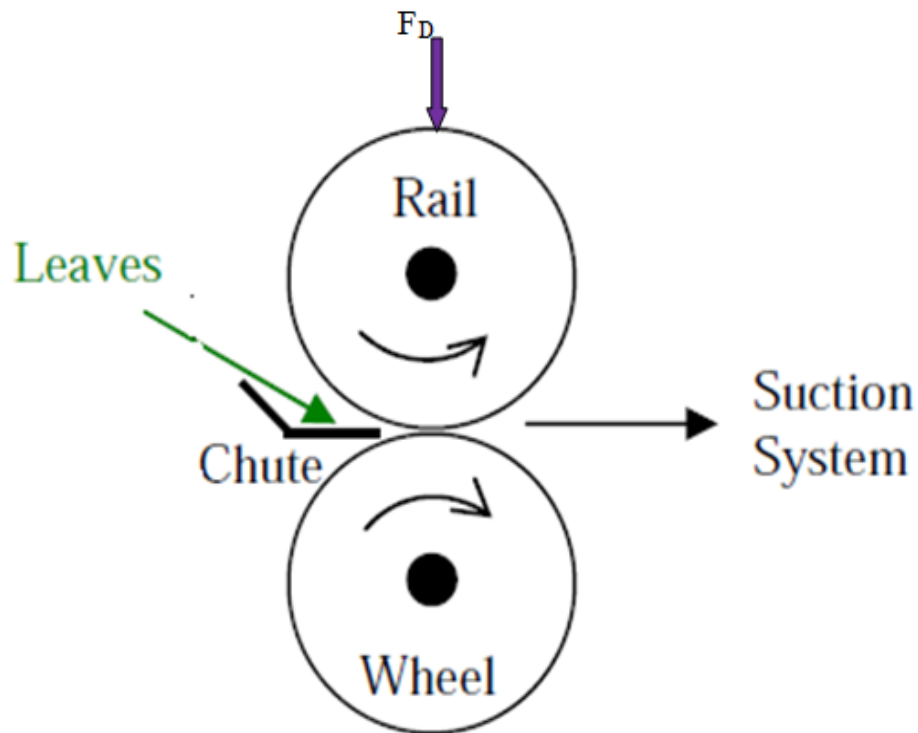


Figure 3.7 Experimental set up of leaves feeding

In each test, equal amount of wet leaves were fed enough to create a relatively hard, durable leaf layer on the disk surface. At the beginning of each test, the disks were run at 0% slip for 2 minutes to condition the surface; then 5-10 minutes were required to apply the necessary amount of leaves. Thus the leaf layer generation as in Figure 3.7 simulated what happens in the real situation, in which repeated wheel passages compact and shear leaves on the top of the rail. As has been done in the preceding tests, data were collected at the end of each leaves test where it was believed the readings in the instrument were quite stable.

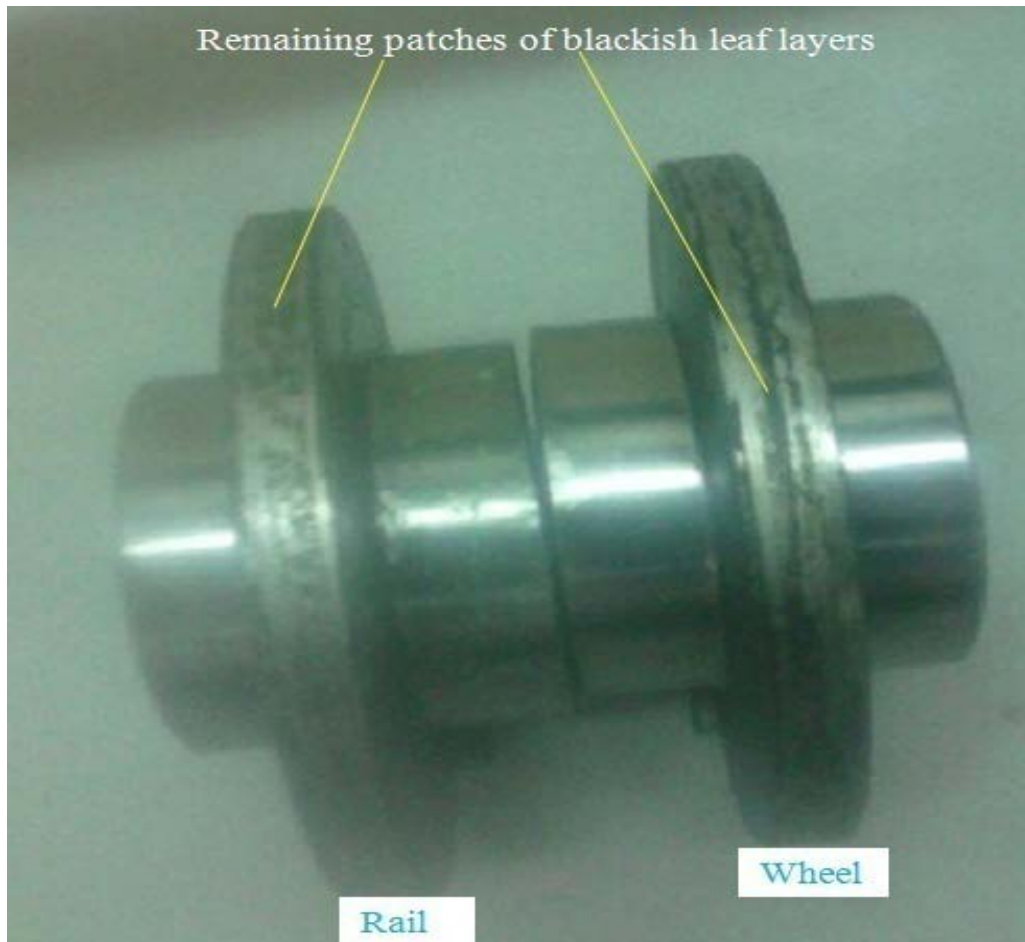


Figure 3.7 Rail and Wheel discs after leaf test with blackish leaf layers

#### IV. Test with oil and grease

Before starting the test with oil, the leaf layer was removed from both discs by rotating against each other dry until the contact surfaces were barely clean. Oil used was standard 15W40 engine oil. For tests with oil, two drops per interval was entertained; the supply was started prior to loading the discs together so the whole test was run lubricated. The test was completed with all the prescribed slip values accomplished and the respective data were collected. To start with grease test, the oily surfaces were first cleaned well with clean rag. At each interval, a paint of grease was applied at the top of rail disc so grease layer was seen to transfer to the wheel disc as the discs persisted running with the load of 400N and data were collected at each test whenever the readings were certainly stable.

## CHAPTERFOUR: RESULT AND DISCUSSION

### 4.1 Experimental Results

#### 4.1.1 Dry tests

The adhesions results for 0, 0.25, 0.5, 1, and 2 to 10% slip in dry conditions are given in Figure. 4.1. The dry test gave the largest adhesion, with adhesion coefficients at 0.58 for the slip value of 3%. The adhesion results as seen in the curve, the maximum adhesion coefficient was observed at 3% slip while in most researches was found to be 0.6 at 2-3% slip. However, this is closely in good agreement with previous researches [3, 14, and 17] carried out with this roller rigs. Furthermore, in all researches the test investigated with dry test at zero slip was seen to be almost zero adhesion i.e. indication of pure rolling but in this particular test it has come to be 0.1. This could be due to the resistance torque of bearing and some misalignment of couplings due imprecision of the test machine and other factors.

Table 4.1 Slip values Vs adhesion coefficient of dry test

Test No	Slip (%)	T calc (Nm)	T const. (Nm)	$\mu_a$ calc
1	0	0.60	6	0.10
2	0.25	0.68	6	0.11
3	0.5	0.93	6	0.15
4	1	1.51	6	0.25
5	2	2.90	6	0.48
6	3	3.50	6	0.58
7	4	3.34	6	0.56
8	5	3.34	6	0.56
9	6	3.39	6	0.57
10	7	3.43	6	0.57
11	8	3.32	6	0.55
12	9	3.26	6	0.54
13	10	3.20	6	0.53

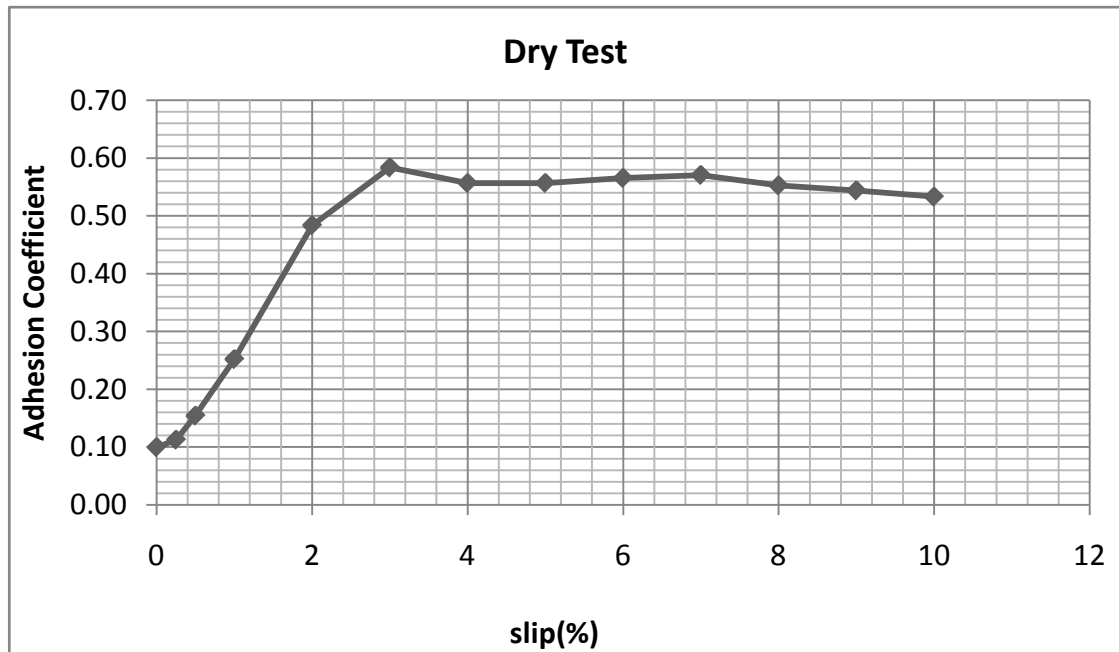


Figure 4.1 Adhesion tests in dry conditions

#### 4.1.2 Water test

Figure 4.2 shows the adhesion results obtained for the tests with water. As soon as water was entrained in the contact, the adhesion coefficient seen to rise to pick at 0.29 and started to decrease after wards as the slip further increased. The lowest value in adhesion coefficient was 0.06 at zero slip while in other researches this was seen to be zero. As described in dry test the reason holds true for this test, too.

Table 4.2 Slip values Vs adhesion coefficient of water test

Test No	slip	T calc	T const	$\mu_a$ calc.
1	0	0.34	6	0.06
2	0.25	0.53	6	0.09
3	0.5	0.93	6	0.15
4	1	1.21	6	0.20
5	2	1.76	6	0.29
6	3	1.72	6	0.29
7	4	1.66	6	0.28
8	5	1.52	6	0.25
9	6	1.50	6	0.25
10	7	1.34	6	0.22
11	8	1.26	6	0.21
12	9	1.23	6	0.20
13	10	1.16	6	0.19

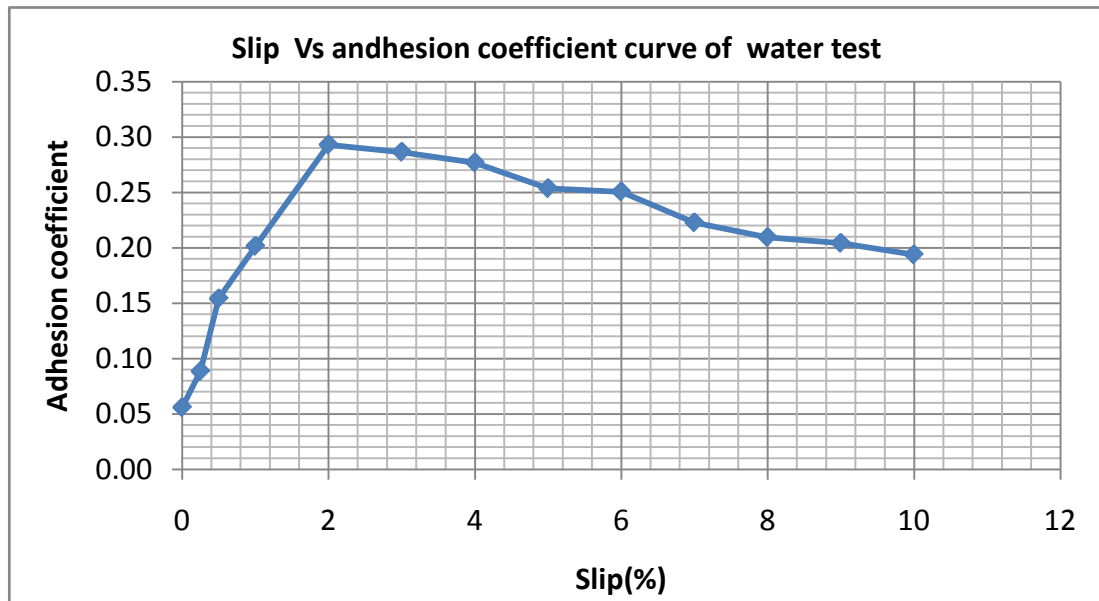


Figure 4.2 Adhesion tests in wet condition conditions

#### 4.1.3 Mud test

Figure 4.3 shows the adhesion results obtained for the mud tests. Here also as mud was entrained in the contact, the adhesion coefficient seen to rise starting from 0.05 to 0.31 pick at 3% slip and started to decrease after wards as the slip further increased but with more irregularities. The lowest value in adhesion coefficient was 0.05 at zero slip. Fine sand grain size in the mud could enhance rolling motion that was why the adhesion at start was a little bit higher than in water test.

Table 4.3 Slip values Vs adhesion coefficient of mud test

Test No	slip	T calc	T const.	$\mu_a$ calc.
1	0	0.29	6	0.05
2	0.25	0.53	6	0.09
3	0.5	0.93	6	0.15
4	1	1.51	6	0.25
5	2	1.68	6	0.28
6	3	1.87	6	0.31
7	4	1.75	6	0.29
8	5	1.68	6	0.28
9	6	1.79	6	0.30
10	7	1.64	6	0.27
11	8	1.85	6	0.31
12	9	1.71	6	0.28
13	10	1.67	6	0.28

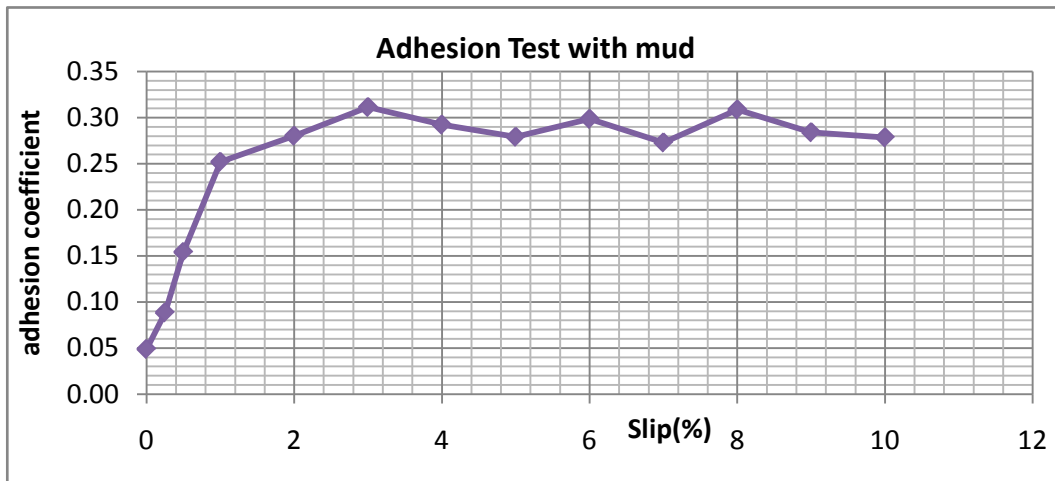


Figure 4.3 Adhesion tests in muddy conditions

#### 4.1.4 Leaf test

During wet leaf tests separate tests at different slip values were run so that a soft dark layer was apparent on the disc surfaces immediately after 5 to 10 minutes (with visible wrinkles), as shown in Figure 3.7 this was relatively easy to remove, but underneath was somehow hard to remove; this layer was responsible for the adhesion loss in the way as depicted in the graph below Figure 4.3. As shown in the graph, at zero slip 0.07 adhesion was registered and peaked 0.43 at slip of 3% and afterwards was seen to decrease steeply as compared to the preceding tests because of the formation blackish layer as slip increased.

Table 4.4 Slip values Vs adhesion coefficient of leaf test

Test No	Slip (%)	T <sub>calc.</sub> (Nm)	T <sub>const</sub> (Nm)	$\mu$ <sub>a</sub> calc.
1	0	0.40	6	0.07
2	0.25	0.53	6	0.09
3	0.5	0.96	6	0.16
4	1	1.38	6	0.23
5	2	2.04	6	0.34
6	3	2.59	6	0.43
7	4	2.37	6	0.39
8	5	2.38	6	0.40
9	6	2.20	6	0.37
10	7	2.03	6	0.34
11	8	1.90	6	0.32
12	9	1.71	6	0.28
13	10	1.70	6	0.28

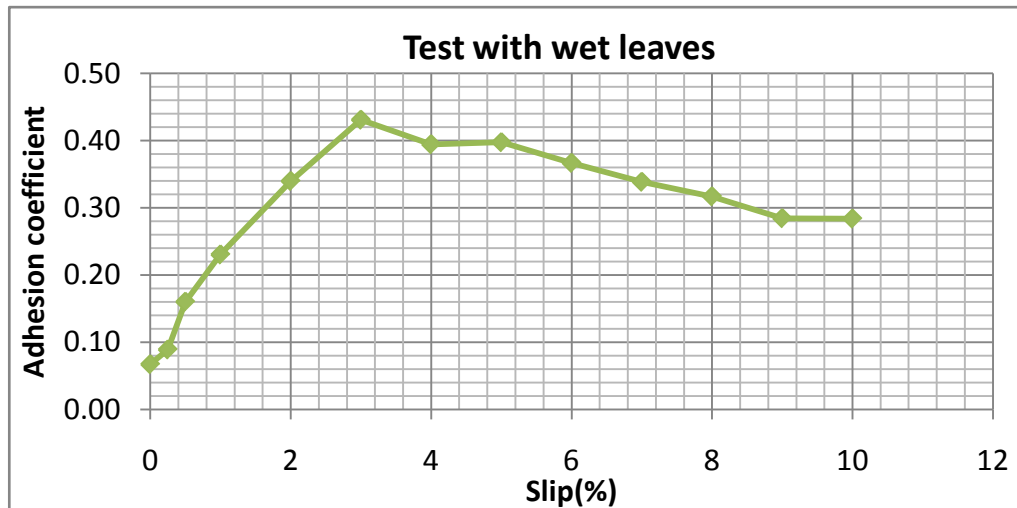


Figure 4.4 Adhesion tests in wet leaves

#### 4.1.5 Test with oil

Similarly, tests with oil were performed with all the slips and at the start of the slip were registered 0.03 and came to pick in 0.09 at 0.5 -1% slip values. The curve was seen less steeply and smooth after wards.

Table 4.5 Slip values Vs adhesion coefficient of oil test

Test No	Slip (%)	Tcalc (Nm)	Tconst (Nm)	$\mu_a$ calc.
1	0	0.19	6	0.03
2	0.25	0.43	6	0.07
3	0.5	0.54	6	0.09
4	1	0.56	6	0.09
5	2	0.55	6	0.09
6	3	0.49	6	0.08
7	4	0.50	6	0.08
8	5	0.49	6	0.08
9	6	0.50	6	0.08
10	7	0.48	6	0.08
11	8	0.45	6	0.08
12	9	0.44	6	0.07
13	10	0.42	6	0.07

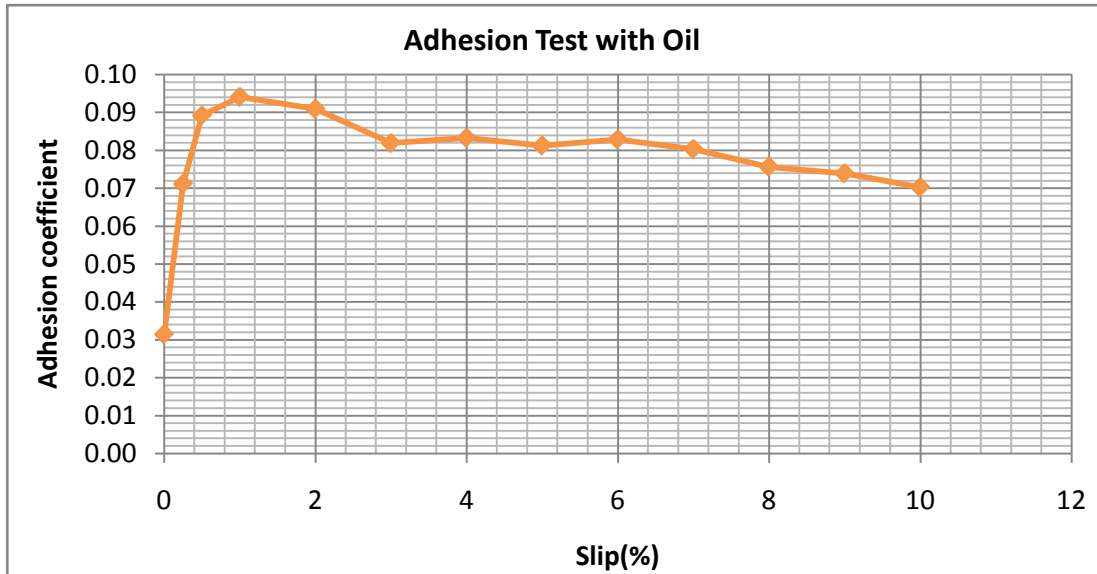


Figure 4.5 Adhesion tests in oil contaminated condition

#### 4.1.6 Test with grease

With similar fashion as oil test, the curve was seen quite similar with a little shift up in the adhesion coefficients compared to oil as seen in the Figure 4.6.

Table 4.6 Slip values Vs adhesion coefficient of grease test

Test No	Slip(%)	T calc.(Nm)	T const (Nm)	$\mu_a$ calc.
1	0	0.27	6	0.05
2	0.25	0.47	6	0.08
3	0.5	0.54	6	0.09
4	1	0.57	6	0.10
5	2	0.53	6	0.09
6	3	0.53	6	0.09
7	4	0.54	6	0.09
8	5	0.53	6	0.09
9	6	0.53	6	0.09
10	7	0.52	6	0.09
11	8	0.50	6	0.08
12	9	0.44	6	0.07
13	10	0.41	6	0.07

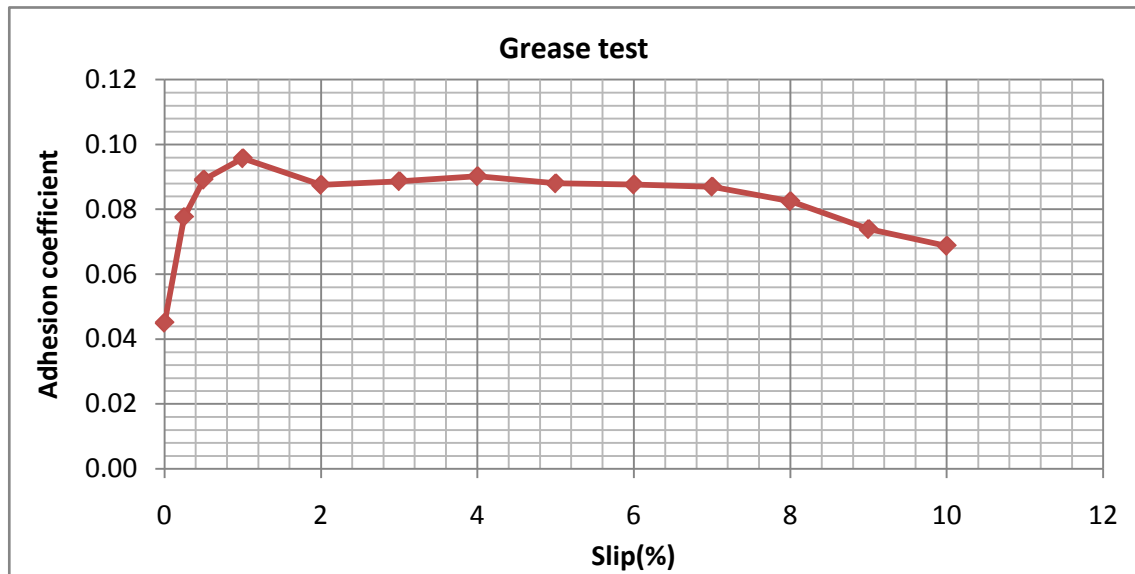


Figure 4.6 Adhesion tests of grease as a contaminant

## 4.2 Discussion

The highest adhesion levels are obtained in dry conditions without contaminant, which are 0.58 for the relative slip 3%. Leaves show the next highest adhesion coefficient with value 0.43. This is in contrary to the researches made so far. As investigated in the literatures [3, 14, 18 and 20] the adhesion due to were found to be lesser than even that of oil. But in this particular thesis work it was found higher than that of water's.

Table 4.7 all adhesion data of the contaminants are collected for comparison purpose

Slip (%)	$\mu_a$ dry	$\mu_a$ (water)	$\mu_a$ (mud)	$\mu_a$ wet (leaves)	$\mu_a$ (oil)	$\mu_a$ (grease)
0	0.10	0.06	0.05	0.07	0.03	0.05
0.25	0.11	0.09	0.09	0.09	0.07	0.08
0.5	0.15	0.15	0.15	0.16	0.09	0.09
1	0.25	0.20	0.25	0.23	0.09	0.10
2	0.48	0.29	0.28	0.34	0.09	0.09
3	0.58	0.29	0.31	0.43	0.08	0.09
4	0.56	0.28	0.29	0.39	0.08	0.09
5	0.56	0.25	0.28	0.40	0.08	0.09
6	0.57	0.25	0.30	0.37	0.08	0.09
7	0.57	0.22	0.27	0.34	0.08	0.09
8	0.55	0.21	0.31	0.32	0.08	0.08
9	0.54	0.20	0.28	0.28	0.07	0.07
10	0.53	0.19	0.28	0.28	0.07	0.07

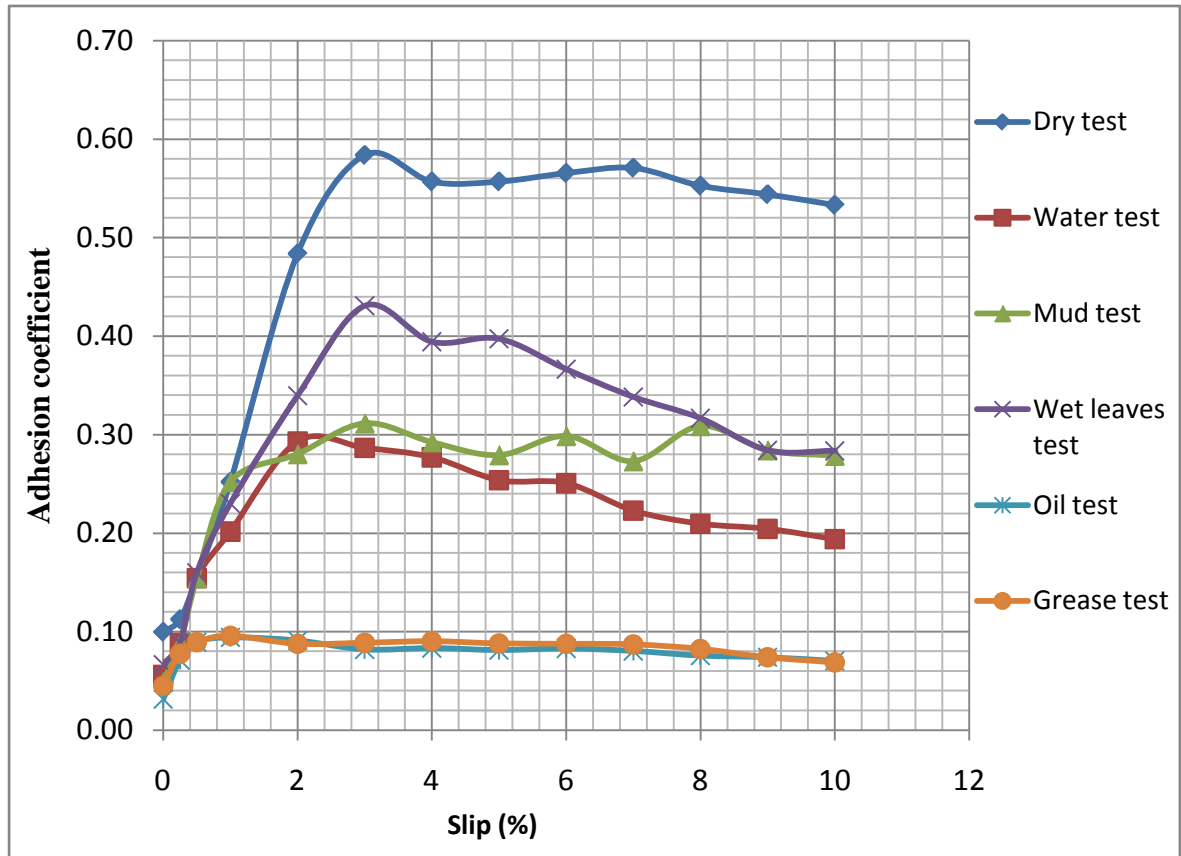


Figure 4.7.Slip/Creep Curves for the various Test Conditions

When water was applied to the discs contact, the adhesion coefficient drops to 0.29 peaks at 2% slip faster recovery than that of mud and dry. The mud test came to peak higher than that of water at 3% slip beneath that of leaf. The largest drop in adhesion was seen with both in the oil and greases as compared to the three contaminants to 0.09 and 0.1, the adhesion coefficient of course at slip of 0.5 and 1% respectively.

The adhesion requirements differ for traction and braking operations and they also depend on the type of vehicle under consideration. An adequate braking performance demands an adhesion up to 0.09, where as in traction, this can be up to 0.20 [31]. Based on this, the low level of adhesion found with oil and grease may primarily lead to traction problems. On the other hand, the moderate adhesion level reached within water would be advantageous to reduce wear and the occurrence of rolling contact fatigue defects in rails subject to high tangential forces, like in accelerating/braking sections and short-radius curves. However, it has to be acknowledged that the adhesion coefficients obtained in this testing may not be completely in agreement with

the actual wheel-rail adhesion, because of the differences between the actual and laboratory testing conditions as already pointed out. Therefore, the results presented in this work can only be taken as qualitative of the actual wheel-rail situation to be used for comparisons between the contaminants tested and the dry test. The influence of water is one of the most important factors to investigate further, as it is recurring in the regular rainy seasons of Ethiopia in which the rain water is expected to exert an influence on adhesion loss because there is an indications in the results attained other than oil and grease it was found adhesion depriving contaminant. In this work, however, wear and indentations are present in both wheel and rail disks, which can be attributed to the small difference in hardness of the wheel and rail steels. Furthermore, the moderate adhesion coefficients obtained with dry conditions lead to less plastic deformation on the disks compared to the lubricated contact. The wear rates were also seen to reduce compared to dry test. These facts would make more beneficial from the railway maintenance point of view if appropriate friction modifiers are applied on sections where the rails experience high tangential forces as indicated above. Nevertheless, in this laboratory test can only be taken as a reference of what happens in the actual wheel-rail contact, as already discussed in the test description part.

# CHAPTER FIVE: CONCLUSION, RECOMMENDATION AND FUTURE WORK

## 5.1 Conclusion

A twin-disk roller rig is used to simulate the wheel-rail contact in somewhat controlled laboratory conditions so as to study the influence of contaminants in consideration and compare with dry contact. These contaminants have been used or tested in several railway networks as adhesion depriving agents. In this work, tests with these contaminants and dry condition were carried out at different slip Values.

Due to the early establishment of railway engineering sector no research has been made in Ethiopia so far on adhesion losses with any of the contaminants in to consideration thus this thesis is the first in attempting an experimental test on the contaminants selected for this work with a twin test machine constructed as part of this thesis.

Uniqueness of this work

The test conditions:

- Load
- speed
- environmental conditions
- Leaves used
- Method of acquiring torque is quite different with previous investigation but the results attained were in good agreement.
- The test rigs are different in dimension and shape but do have the same contact width

Conclusions drawn from the test results:

- a) In dry conditions the highest adhesion coefficients are obtained at 3% with a value of 0.58 which is in good agreement with previous investigations made. Dry test as was expected higher, wear debris was collected, indication of high wear.
- b) Water test seen moderate at lower slip but declined after peak, indication of worse condition for adhesion; will be even worst combined with other contaminants.
- c) The leaf layer generation simulated what happens in the real situation, in which repeated wheel passages compact and shear leaves on the top of the rail. In the presence of water the adhesion coefficient is reduced to 0.29, whereas 0.31 for mud. The later may primarily lead to a conclusion that it was higher because the mud may contain fine sand particles that enhanced the adhesion coefficient.
- d) Mud and leaves were seen to have same effect at higher slip by filling the grooves in between asperities. As the slip increased further the effect of mud was seen to be on line with that of leaves as seen in the curve figure 5.7. As discussed in the discussion part of this paper, the adhesion loss caused in leaf test was due to the black leaf layer adhered on the contact surface filling the grooves of the asperities; likely due to the contact temperature the dried mud adhered in between asperities causing the same effect as that of leaves.
- e) Both the oil and grease leads to a faster recovery time and lowest adhesion of all the contaminants for all the slip values considered. The increase in slip led a to stable adhesion loss rather significantly declining. Therefore, the use of more adequate track side lubrications may lead to an undesirable adhesion loss extent to the wheel rail contacts.
- f) In the investigations made so far , at 0% slip ,creep curves starts from origin but in this work is other than zero due to the inherited resistances (bearing, misalignment, vibration etc.) exerting torque

## 5.2 Recommendation

- From the result found, experimental method of assessing adhesion loss is the best way with twin disc test machine. The test results would have been in best agreement with previous investigations had servo motors and measuring devices been fitted to the test machine.
- Had the shunt motors been good capacity, it could have been possible to simulate the contact pressure close to the real situation of the railway system
- According to the experiment, oil and grease were seen to produce the lowest extent of adhesion. Thus mal- function of rail edge and wheel flange lubrication mechanisms may cause severe adhesion loss due to the migration of this lubrication to the rail head. Therefore, Internal and track side lubrication appliances should be frequently checked for their proper functions.
- In this particular experiment, wet test result seemed moderate for both traction and braking. But as to the real situation of the rail-wheel contact condition, the result triggers this could be even least if all the conditions were fulfilled. Therefore, in the rainy seasons, rain can affect significant lengths of track, as can dew or other condensation effects thus train should be equipped with adhesion enhancer or modifier so as to ensure safety and full utilization of the capacity of the rolling stock. For safe and reliable operation of the rolling stock, rail head should often be clear of mud and leaves because there is an indication that these contaminants can cause adhesion problems.
- Train operators should be given awareness about the effects of contaminants and the measures that should be taken whenever they are faced.

### 5.3 Future Work

The machine developed does have limitations up on simulating with the real situation of railway system as SORUS and Amasler research centers' Twin disc test machine.

Finally, some suggestions are listed below for future work as extension and continuity of this paper.

- Load application was limited to 120N because of the capacity of the shunt type motor availed.
- Due to unavailability of DC servo motors, data feeding and collection were made manually. Had these motors been found all data feeding and collection would have been well controlled through personal computer. The data collected also could have been directly presented graphically. For the future this machine will be equipped with these mentioned types of motors and adhesion experiments will be performed so that the results will be in best agreement with the tests made so for by different researchers.
- Some other contaminant such as:
  - Plastic bags with different thickness simulating used 'festal' from thinnest to thicker layer mostly clogging the track side environments.
  - Wear debris
  - Rust and other related track side contaminants will be assessed and tested in the future.

## Reference

- [1] Yi Zhu, Adhesion in the wheel–rail contact under contaminated conditions, 2013
- [2] Yi Zhu, Adhesion in the wheel–rail contact under contaminated conditions, 2011
- [3] Oscar Arias –Cuevnans, Low Adhesion In the wheel-rail contact, 2010
- [4] Daniel Frylmark and Stefan Johnsson, Automatic Slip Control for Railway Vehicles, February 2003
- [5] Dipl.-Ing. Charles-Alix Manier, Slip-rolling resistance of novel Zr (C, N) thin film coatings under high Hertzian contact Pressures, 2010.
- [6] J. De Pauw, J. Van Wittenberghe, P. De Baets, Traction and Wear Mechanisms during Roll-Slip Contact, February 2010
- [7] Rail Accident Investigation Branch (RAIB)( Department for Transport), Review of adhesion-related incidents during autumn, 2007
- [8] E.A. Gallardo-Hernandez, R. Lewis, Twin Disc Assessment of Wheel/Rail Adhesion, 2008, *Wear*, 265 (9-10). pp. 1309-1316
- [9] Jaakko Kleemola, Experimental methods for the evaluation of lubrication conditions in gear contacts, 20110
- [10] G.Vasic, F.J.Franklin&A.Kapoor, New rail materials and coating, July 2003
- [11] J.Y. Choi, I.Y. Choi, J.S. Lee, T.W. Kim D.H. LEE, J.W. Seo, Development of high speed rail-wheel contact simulator,2011
- [12] Nicola Bosso and Nicolò Zampieri , Experimental and Numerical Simulation of Wheel-Rail Adhesion and Wear Using a Scaled Roller Rig and a Real-Time Contact Code, 23 February 2014
- [13] H. Chen, M. Ishida, T. Nakahara, Influential Factors on Adhesion between Wheel and Rail under Wet Conditions, May 2011
- [14] Kenza Ikoubel, Twin disc testing as a method of evaluation of rolling contact

- [15] Min-Soo Kim And Nam-Po Kim, Design of the Scaled Adhesion Tester for Analyzing the Adhesion Characteristic of Railway Vehicle, pp.129-132
- [16] Radim Halamaa, Rostislav Fajkošb, Petr Matušekb, Petra Bábkovác, František Fojtíka, Leo Václaveka, Contact Defects Initiation In Railroad Wheels –Experience, Experiments And Modeling, Wear. 2011, vol. 271, issue 1-2, p. 174-185
- [17] Anneli Orvans, Simulation of Rail Wear on Swedish Light Rail Line Tvarbanan, March 2005
- [18] Rail Safety and Standards Board, Guidance on Wheel / Rail Low Adhesion Simulation, February 2008
- [19] Arias-Cuevas, O., Li, Z., Lewis, R., Gallardo-Hernandez, Rolling sliding laboratory tests of friction modifiers in dry and wet wheel-rail contacts, 2010.
- [20] Arias-Cuevas, O., Li, Z., Lewis, R., Gallardo-Hernandez Rolling–Sliding Laboratory Tests of Friction Modifiers in Leaf Contaminated Wheel–Rail Contacts, November 2008 268 (3-4), pp. 543-551
- [21] Meehan P.A., Bellette P., Liu X., Milne C. & Anderson D., Investigation of Wheel Squeal Characteristics using a Rolling Contact Two Disk Test Rig, May 2011
- [22] Lance Jon Wilson, Performance Measurements of Rail Curve lubricants, 2006.
- [23] Maksym Spiriyagin, Kwan Soo Lee<sup>1</sup>, Hong Hee Yoo, Valentyn Spiriyagin and Yuriy Vivdenko, Experimental And Theoretical Investigation of adhesion Based On Analysis Of Wheel-Rail Noise, 2008
- [24] Yosuke Takaoka, Keiichi Takeuchi, Takemasa Furuya, Kantaro Yoshimoto, Yokohama National University, Japan, Measurement of Tractive Force in the Creep Region and Maximum Adhesion Control of High Speed Railway Systems fatigue in cam ring steel
- [25] H.M.A. Smetsers, Applying a CVT in a two roller test machine, August 2006
- [26] Hsu, Z Huang, S D Iwnicki<sup>1</sup>, D J Thompson, C J C Jones, G Xie<sup>1</sup>, and P D Allen Experimental and theoretical investigation of railway wheel squeal, September 2007 pp. 59-73.

- [27] L. Chevalier, S. Cloupet, M. Quillien, Friction and Wear during Twin-disc Experiments under Ambient and Cryogenic Condition, 2005
- [28] Maksym Spiryagin , Kwan Soo Lee , Hong Hee Yoo , Oleksandr Kashura and Oleksandr Kostyukevich , Modeling of Adhesion for Railway Vehicles, August 2007
- [29] J V Ardelean, R Malik, A V Navratil, J P Kyle, S K Wilkinson, and E J Terrell, Influence of Slide-to-Roll Ratio and Contact Radius on Traction in Lubricated Roll-Slide Line Contacts, Nov 2013
- [30] R.B. van Iperen , The application of a CVT in a Two Disc Test Machine, August 2006
- [31] Zili Li, Oscar Arias-Cuevas, An investigation on the Desired Properties of Friction Modifiers for Slippery Rails, 2009
- [32] Yusuf Caner Tasan, Measurement of Deformation in Rolling and Sliding Contacts, July 2005
- [33] E.J. M. Hiensch, A.Kapoorb, B.L.Josefsonc, J.W.Ringsbergc, J.C.ONielsenc and F.J.Franklin, Two-Material Rail Development to Prevent Rolling Contact Fatigue and to Reduce Noise Levels in Curved Rail Track, December 2003
- [34] G. I. Crabb, S Brown, P. D Sanders, D. Wright, S McRobbie and H.Viner, Investigation of novel systems for monitoring rail adhesion, 2013
- [35] Rail Safety and Standards Board, Review of Low Adhesion Research, May 2004
- [36] Ulf Olofsson and Roger Lewis, Tribology of the Wheel-Rail Contact, 2006, pp.121-138
- [37] R.S. Dwyer-Joyce, R. Lewis, N. Gao and D.G. Grieve, Wear And Fatigue Of Railway Track Caused By Contamination, Sanding And Surface Damage
- [38] N. Tassini , X. Quost, R. Lewis, R. Dwyer-Joyce, C. Ariaudo, N. Kuka , A Numerical Model Of Twin Disc Test Arrangement For The Evaluation Of Railway Wheel Wear Prediction Methods,2010, Wear, 268 (5-6), pp. 660-667

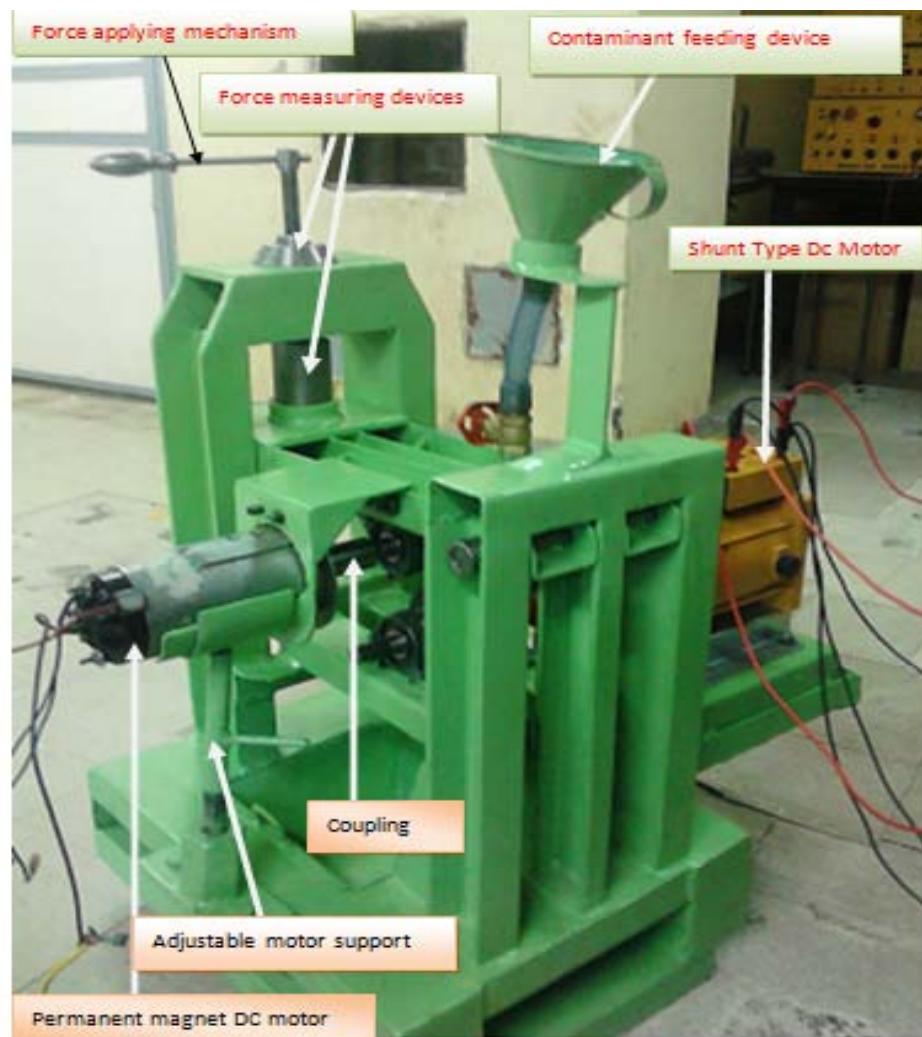
## Appendix

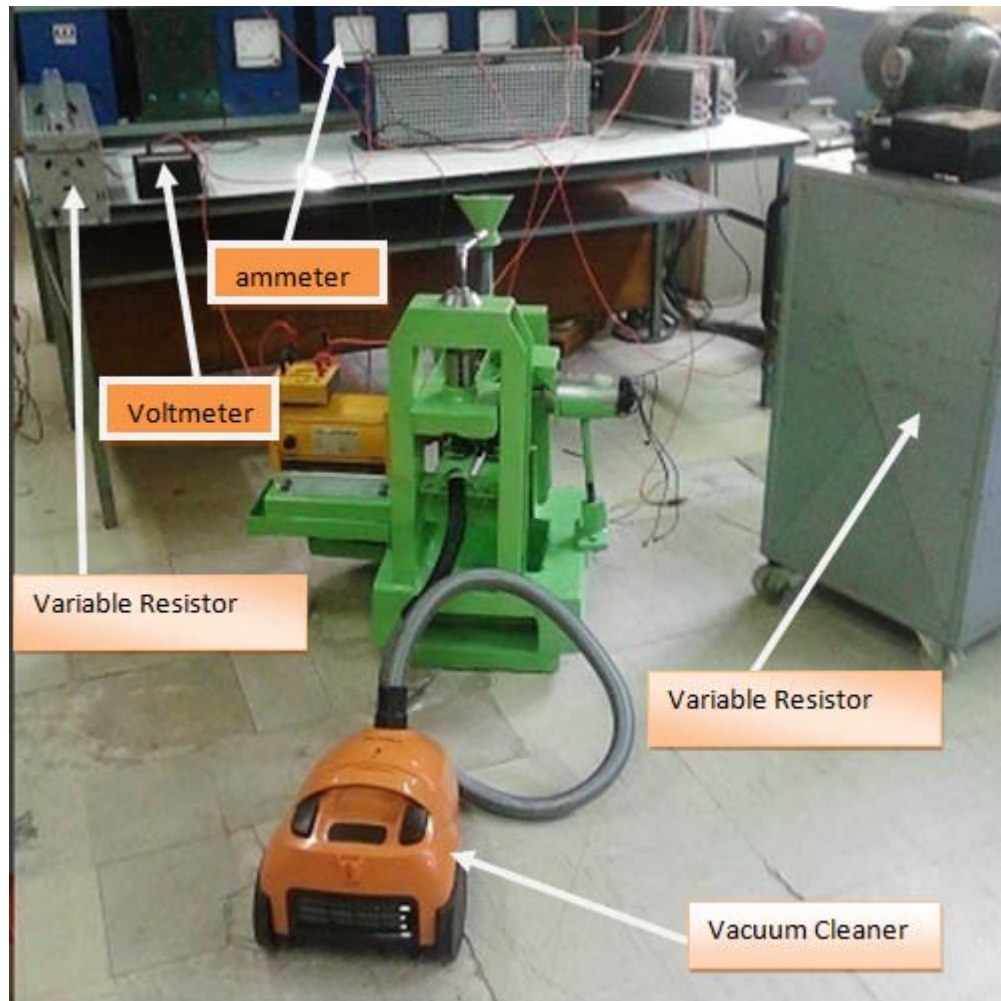
### Adhesion Testing Apparatus/Twin disc test machine

#### Function and layout

The most commonly used equipment for investigating wheel–rail adhesion under various conditions is the twin-disc machine. Because the twin-disc machine can generate rolling–sliding contact, it can simulate the motion of the wheel on the rail.

Two independent motors (shunt type with capacity of 0.3KW and Permanent magnet DC motor with 2.65 Hp) each of which is capable of transmitting a torque to couple the twin discs each other so as to rotate them to the required speed creating an intended slip velocities. A speed is read with a speed sensing speedometer and torque is calculated from the armature voltage and current read from the ammeter and voltmeter respectively at each application of the contaminant.





The specimens/test rigs are two steel rollers tangentially positioned against each other in rolling –sliding contact. The discs rotate in opposite directions. These independently driven discs pushed against each other with a constant applied load ( $F_{app}$ ). The inputs are the applied normal contact load and the slip /creep between the two discs while the outputs are the tangential force/torque whose the basis for calculating adhesion coefficients under different contaminants. This tangential force (adhesion or breaking) is the main parameter to compare the different contaminants causing adhesion losses in the real wheel-rail contact with an adhesion coefficient calculated from the tangential force to normal force between the two contacting discs. The machine is composed of three main parts: Mechanical part, electrical part and measuring equipments.

The Mechanical part comprises a horizontally lied load lever which can multiply the applied load to the discs, in the mean time supporting the wheel disc/specimen and the

upper motor. The discs are in turn supported by two shafts axially parallel to each other which in turn supported by the bearings. Main vertical frame supporting the load mechanism (T- bolt) , sub-vertical frame/pivot frame holding the pivot pin are some of the mechanical parts. The motor shafts which drive the wheel discs are coupled with the wheel disc shafts by couplings.

**ADDIS ABABA UNIVERSITY****ADDIS ABABA INSTITUTE OF TECHNOLOGY****SCHOOL OF MECHANICAL AND INDUSTRIAL ENGINEERING****DECLARATION**

I, the undersigned, declare that this thesis is my original work and has not been presented for any degree in any university and all the sources of materials used for the thesis have been duly acknowledged.

Mesfin G/Tsadik

Name

Signature

Date